Supplement: The Chern Theorem and High-Spin Topological States in Nuclear Structure Physics

Mike Guidry and Yang Sun

This document provides supplemental material and proofs of some important equations for the article "Conjectured High-Spin Topological States in Nuclear Structure Physics" by Mike Guidry and Yang Sun, published in the journal *xxxx* (2024).

I. INTRODUCTION

In the following all citations of sections, subsections, equation numbers, figure numbers, and table numbers are by default references to the primary document "Conjectured High-Spin Topological States in Nuclear Structure Physics" published by the present authors in the journal *xxxx* (2024). If a reference is flagged by "[this document]", it is instead a reference to objects in the present Supplement document.

II. THE INTEGER QUANTUM HALL EFFECT

We take as prototype the integer quantum Hall effect (IQHE) for 2D electron gases in strong magnetic fields that is illustrated in Fig. 1 [this document], and the explanation of the quantized Hall resistance observed there in terms of the Chern theorem. In the IQHE this identification leads to the TKNN formula [5]

$$\sigma_{\rm H} = C_1 \frac{e^2}{\hbar} \tag{1}$$

Note that the Hall resistance $R_{\rm H}$ that is plotted in Fig. 1 [this document] is related inversely to the Hall conductance $\sigma_{\rm H}$ calculated in Eq. (1) [this document]: $R_{\rm H} = \sigma_{\rm H}^{-1}$.)

For the integer quantum Hall effect (IQHE) displayed in Fig. 1 [this document], it is found that the precise quantization of the observed Hall resistance plateaus (as good as a part in a billion) can be explained by the Chern theorem. Before the topological interpretation of the IQHE, it was understood qualitatively how filling of Landau levels could lead to the observed plateaus for the Hall resistance. What could not be explained was the remarkable flatness of the plateaus, given that an experimental device is averaging over many configurations as the magnetic field is varied, and that the results are found to be robust across different device specifics. What was needed was a principle that *quantized averages of quantum matrix elements.* The Chern theorem provided that missing link.

The plateau structure observed for the integer quantum Hall effect becomes strongly defined only at larger values of the magnetic field strength. As illustrated in Fig. 1 [this document], at low magnetic fields the Hall resistance exhibits the linear dependence on B characteristic of the classical Hall effect. Only above about $B \sim 1$ T does the Hall resistance begin to develop step structure deviating from the classical expectation, and these steps become better defined as B increases. Since rotational angular momentum is the analog of magnetic field in the present discussion, we may expect that the implications of Eq. (23) become better defined for large average angular momentum.

III. THE GAUSS–BONNET AND CHERN THEOREMS

For a 2D surface there is a relationship between its geometry and its topology called the *Gauss–Bonnet theorem,* which may be expressed through the *Gauss–Bonnet equation,*

$$\frac{1}{2\pi}\int_S K dA = 2(1-g), \tag{2}$$

where the integral is over a closed surface S, the local curvature is K, and g is the genus of the surface (number of "holes", which characterizes its topology). The Gauss–Bonnet theorem relates the geometrical properties of the 2-surface (local curvature K on the left side) and its topological properties (the genus g on the right side), with g a *topological invariant* because the number of holes is not changed by smooth deformations of the surface. The 2D manifolds displayed in Fig. 2 [this document] illustrate.

A fundamental implication of Eq. (2) is illustrated in Fig. 3 [this document]. The integer $2(1-g)$ on the right side of Eq. (2) cannot change continuously into another integer for a small, smooth deformation of the surface, which implies that *the integral on the left side cannot change either.* Thus, in Fig. 3 [this document] the left side is *topologically protected* against change for smooth deformations that do not change the genus.

The Gauss–Bonnet equation (2) relates geometry and topology for 2-surfaces, but S.-S. Chern generalized the Gauss–Bonnet equation to the *Gauss–Bonnet–Chern equation* (which for brevity we will term the *Chern equation*),

$$\frac{1}{2\pi}\int_S \Omega\, dA = C_n. \tag{3}$$

This resembles the Gauss–Bonnet formula (2), except that for n a positive integer,

1. Equation (3) holds for any $2n$-dimensional Riemannian manifold.

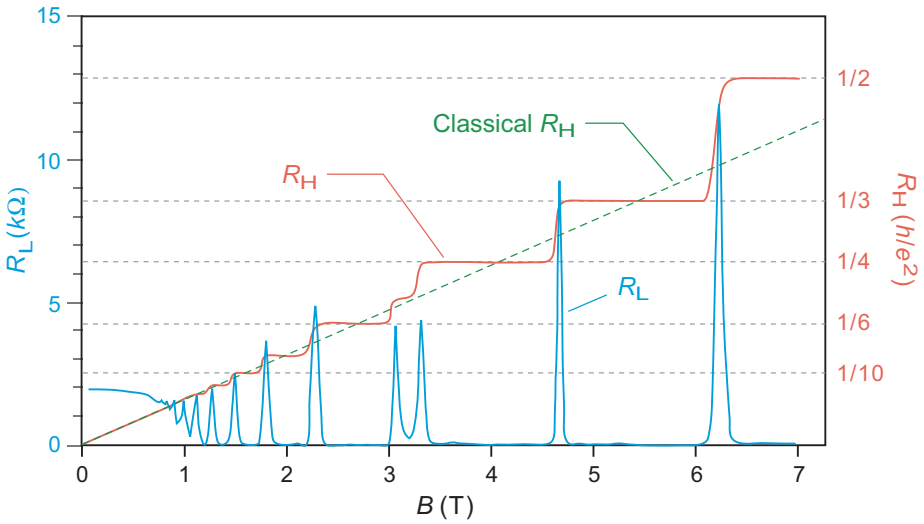

FIG. 1: Data illustrating the integer quantum Hall effect [6]. The Hall resistance R_H (red upper curve) is equal to the inverse of the Hall conductance σ_H defined in Eq. (1), and varies stepwise with changes in magnetic field strength B. Step height is given by the physical constant h/e^2 divided by an integer. The lower blue curve with multiple peaks is the longitudinal resistance R_L, which essentially vanishes over each plateau in R_H. The dashed green curve is the linear behavior of R_H expected from the classical Hall effect; obvious deviations from the classical curve in the form of plateaus appear above $B \sim 1$ T. The plateaus in R_H are flat to as much as a part in a billion. Figure adapted from Ref. [9].

2. The *Berry curvature* Ω is evaluated over a manifold of quantum states (Hilbert space) defined on S.

3. The *Chern index* C_n in Eq. (3) is an integer that labels a *Chern class*. It is determined by *the topology of a manifold of quantum states (the Hilbert space)* defined over S.

For 2D manifolds the index C_n is a *Chern number of the first kind* C_1, which takes values from the set of integers Z. General implications of Eq. (3) will be termed the *Chern theorem.*

Chern theorem: The integral of Berry curvature over a closed manifold of quantum states is quantized in terms of topological Chern numbers that take integer values.

By analogy with the Gauss–Bonnett equation (2) and Fig. 3 [this document], one finds that Eq. (3) is *topologically protected* under smooth deformations that do not change the Chern number on its right side; the Chern number can be changed only by a *phase transition* to a state that differs topologically from the original state. This topological protection accounts for the the remarkable flatness of the plateaus exhibited by the integer quantum Hall effect in Fig. 1 [this document].

FIG. 2: (a) The 2D sphere has no holes and thus has genus $g = 0$. (b) The 2D torus has one hole and thus has genus $g = 1$. Adapted from Ref. [9].

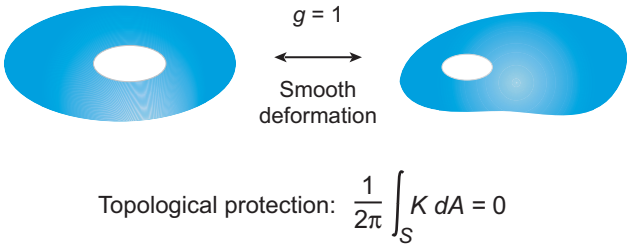

FIG. 3: Smooth deformations that do not change the genus g cannot change the Gauss–Bonnet topological invariant defined by the curvature K integrated over the surface in Eq. (2) [this document]. The curvature may be changed locally by a smooth deformation but the value of $\int_S KdA$ is *topologically protected* if the deformation does not alter the genus for the surface by puncturing or gluing. Adapted from Ref. [9].

General introductions to topological properties of the quantum Hall effect are given in Ref. [10] and in Ch. 28 of Ref. [9]. For a more mathematical discussion of Chern classes in physics, see Frankel [8] or Nakahara [7].

For 2D Hilbert spaces, $n = 1$ and the corresponding Chern numbers $C \equiv C_1$ take values from the set of integers Z. In this paper we will deal only with 2D ($n = 1$) manifolds and sometimes refer loosely to $C \equiv C_1$ as just the Chern number. The essence of the Chern theorem is that Eq. (4) can be *evaluated in two ways*, with results that *must be commensurate*, as illustrated schematically in Fig. 4 [this document].

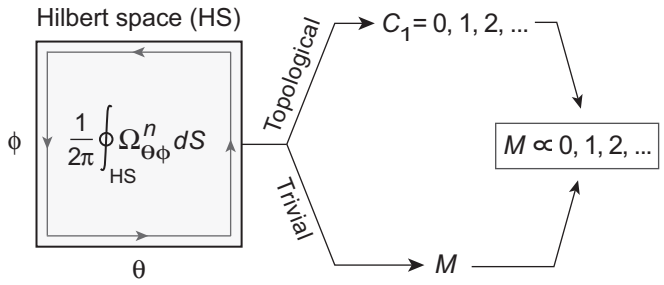

FIG. 4: Chern quantization for a closed 2D Hilbert space. The Berry phase is generally a *geometrical object* taking continuous values, but the Berry phase integrated specifically on a path enclosing the Hilbert space in Eq. (4) is *topological* and required by the Chern theorem to be quantized (the branch labeled "Topological"). The left side of Eq. (4) can also be evaluated by normal quantum-mechanical means assuming the Hilbert space to have trivial topology (the branch labeled "Trivial"). Equivalence of the quantities evaluated by the "Topological" and "Trivial" methods is implied by the Chern theorem, leading to topological quantization of M. Note that the integral over the Hilbert space has been divided by 2π to give integer quantum numbers.

1. If the Hilbert-space manifold is 2D Riemannian, then (independent of details) the *Chern theorem* requires the Berry phase integrated over the entire Hilbert space to be *quantized*, $\gamma_{\rm HS} = 0, 2\pi, 4\pi, \ldots$, in terms of integer Chern numbers, C_1. This is the branch labeled "Topological" in Fig. 4 [this document].

2. Next, evaluate the integrals in Eq. (4) using *ordinary quantum mechanics* assuming *trivial topology* for Hilbert space,

$$M = \oint_{\rm HS} \Omega^n_{\theta\phi} dS, \tag{4}$$

where the Berry curvature tensor Ω may be calculated using nuclear eigenstates. This is the branch labeled "Trivial" in Fig. 4 [this document] (meaning that it is formulated on a Hilbert-space manifold assuming *trivial topology*). The quantity M resulting from this calculation is possibly measurable and in general would be expected to take *continuous values* (it is a geometrical phase, which isn't quantized). This is the analog of evaluating the Hall conductance $\sigma_{\rm H}$ in Eq. (1) [this document] using linear response theory in the IQHE problem.

But the two methods described in points 1 and 2 above each give solutions of Eq. (4) so *their results must be commensurate*, implying that M is proportional to an integer, $M \propto C_1 \propto \{0, 1, 2, \ldots\}$, which restricts the (possibly measurable) quantity M to *quantized values* that are *topologically protected*. In the IQHE this identification leads to the TKNN formula [5], $\sigma_{\rm H} = C_1 \frac{e^2}{\hbar}$ given in Eq. (1) [this document] for the Hall conductance $\sigma_{\rm H}$ (evaluated, for example, using linear response theory), which attributes the remarkable flatness of the IQHE plateaus in Fig. 1 [this document] to this topological quantization.

In summary, the basic methodology of Chern topological quantization is to (1) establish that the Hilbert space manifold satisfies the Chern theorem, (2) compute M by standard quantum mechanics from Eq. (5), assuming trivial topology for the Hilbert space, and relate it to observables, and (3) restrict M to quantized values by equating it to a multiple of a Chern number through the Chern theorem. This is the methodology leading to the topological interpretation of the integer quantum Hall effect, and is the methology that we adopt here to identify possible nuclear topological phases.

IV. BERRY PHASE, CONNECTION, AND CURVATURE

This section gathers important equations for Berry phases, Berry connections, Berry curvature, and their relationship with Chern numbers. To be definite quantities are assumed to be evaluated in a condensed matter Brillouin zone parameterized by momenta $\boldsymbol{k}$, and Bloch wavefunctions $|u_{n\boldsymbol{k}}\rangle$, where n is a band index.

A. Berry connection

The *Berry connection* or *Berry potential* $A^n_\mu(\boldsymbol{k})$ is defined by

$$A^n_\mu(\boldsymbol{k}) = \langle u_{n\boldsymbol{k}} | i\partial_\mu | u_{n\boldsymbol{k}} \rangle, \tag{5}$$

where n is a band index, μ is the index for coordinate x_μ, and $\partial_\mu \equiv \partial/\partial x_\mu$. Equation (5) [this document] may also be written in vector form

$$\boldsymbol{A}^n(\boldsymbol{k}) = \langle u_{n\boldsymbol{k}} | i\nabla_{\boldsymbol{k}} | u_{n\boldsymbol{k}} \rangle. \tag{6}$$

By analogy with electromagnetism, a *gauge transformation* corresponding to a local phase rotation on the wavefunction may be implemented and it is assumed that physical quantities must be gauge invariant. The Berry connection is *not gauge invariant*.

B. Berry phase

The *Berry phase* γ^n may be written as an integral of the Berry curvature over the surface $\boldsymbol{S}$ bounded by the contour C,

$$\begin{aligned}\gamma_n &= \oint_C d\boldsymbol{k} \cdot \boldsymbol{A}_n(\boldsymbol{k}) \\ &= \int_{\boldsymbol{S}} \left(\nabla_{\boldsymbol{k}} \times \boldsymbol{A}_n(\boldsymbol{k})\right) \cdot d\boldsymbol{S} \\ &= \int_{\boldsymbol{S}} \boldsymbol{\Omega}_n(\boldsymbol{k}) \cdot d\boldsymbol{S} \qquad (\text{mod } 2\pi),\end{aligned} \tag{7}$$

where Stokes' theorem was applied in the second line, n is a band index, and mod 2π indicates that γ_n is a phase that is defined up to multiples of 2π. This can also be expressed as

$$\begin{aligned}\gamma_n &= \oint_C \langle u_{n\boldsymbol{k}} | i\partial_\mu | u_{n\boldsymbol{k}} \rangle d\boldsymbol{k} \\ &= \int_S \left(\partial_\mu A^n_\nu(\boldsymbol{k}) - \partial_\nu A^n_\mu(\boldsymbol{k})\right) d\boldsymbol{k}\end{aligned} \tag{8}$$

where C is a contour around the Hilbert space and S is the surface enclosed by that contour. The Berry phase is *gauge invariant* if interpreted as a phase modulo 2π.

C. Berry curvature

The *Berry curvature* $\Omega^n_{\mu\nu}(\boldsymbol{k})$ is defined as

$$\begin{aligned}\Omega^n_{\mu\nu}(\boldsymbol{k}) &= \partial_\mu A^n_\nu(\boldsymbol{k}) - \partial_\nu A^n_\mu(\boldsymbol{k}) \\ &= -2\,\mathrm{Im}\left\langle \partial_\mu u_{n\boldsymbol{k}} \right| \partial_\nu u_{n\boldsymbol{k}} \rangle, \end{aligned} \tag{9}$$

where the Berry connection $A^n_\mu(\boldsymbol{k})$ is defined in Eq. (5) [this document] and Im denotes the imaginary part. In 3D the Berry curvature can also be expressed in pseudovector notation as

$$\boldsymbol{\Omega} = -\mathrm{Im}\langle \nabla_\lambda u| \times |\nabla_\lambda u\rangle \tag{10}$$

If one works in a complete basis, the Berry curvature also may be expressed as

$$\boldsymbol{\Omega}_n(\boldsymbol{R}) = \mathrm{Im}\sum_{m\neq n} \frac{\langle n,\boldsymbol{R}|\nabla_{\boldsymbol{R}} H(\boldsymbol{R})|m,\boldsymbol{R}\rangle \times \langle m,\boldsymbol{R}|\nabla_{\boldsymbol{R}} H(\boldsymbol{R})|n,\boldsymbol{R}\rangle}{[E_n(\boldsymbol{R}) - E_m(\boldsymbol{R})]^2}, \tag{11}$$

where $|n,\boldsymbol{R}\rangle$ are energy eigenstates with n a band index and $\boldsymbol{R}$ the coordinates, the symbol $\times$ indicates the 3-vector cross product, $H(\boldsymbol{R})$ is the Hamiltonian, and Im indicates the imaginary part. The Berry curvature is *gauge invariant*.

D. The Chern theorem

As discussed in Section III [this document], the *Chern theorem* is defined through the Chern equation,

$$\frac{1}{2\pi}\int_S \Omega dS = C_n, \tag{12}$$

where Ω is the Berry curvature of Eqs. (9)-(11) [this document] evaluated for a manifold of states defined over the surface S, and C_n is the Chern number associated with the nth Chern class. For example, $n = 1$ in 2D and in that case the Chern numbers C_1 take values from the set of integers Z.

V. INTRINSIC NUCLEAR STATES

This section considers the relationship of deformed, intrinsic nuclear states to measured laboratory states of good angular momentum that is depicted in Fig. 5 [this document]. We proceed from a general point of view using the method of generator coordinates, following the presentation in Section 22.3.2 of Ref. [9].

A. Representation of Collective Rotational States

Suppose that $|\Phi_0\rangle$ is a deformed state obtained as a solution of some variational calculation for a many-particle system. In general $|\Phi_0\rangle$ is an intrinsic state that violates rotational invariance and hence is not an eigenstate of angular momentum.

1. Generator Coordinate Wavefunction

Define a rotation operator,

$$D(\Omega) = e^{-\imath\alpha J_z} e^{-\imath\beta J_y} e^{-\imath\gamma J_z} = e^{-i\boldsymbol{J}\cdot\boldsymbol{\Omega}}, \tag{13}$$

where $J_i (i = x,y,z)$ are angular momentum operators and $\Omega = (\alpha,\beta,\gamma)$ denotes Euler angles. If the Hamiltonian H is rotationally invariant it commutes with the rotation operator,

$$D^\dagger(\Omega) H D(\Omega) = H. \tag{14}$$

The matrix elements of $D(\Omega)$ for states of good angular momentum are

$$\langle \mu JM|D(\Omega)|\nu JK\rangle = \delta_{\mu\nu} D^J_{MK}(\Omega)^*, \tag{15}$$

where $D^J_{MK}(\Omega)^*$ are the usual Wigner D-functions, which obey the orthogonality condition

$$\int_\Omega D^I_{MM'}(\Omega)^* D^J_{NN'}(\Omega)\, d\Omega = \frac{8\pi^2}{2I+1}\,\delta_{MN}\delta_{M'N'}\delta_{IJ}, \tag{16}$$

with $\Omega = (\alpha,\beta,\gamma)$ and $d\Omega \equiv \sin\beta d\beta d\alpha d\gamma$, It follows that the action of the rotation operator on an angular momentum state $|\nu JK\rangle$ is

$$D(\Omega)|\nu JK\rangle = \sum_M |\nu JM\rangle D^J_{MK}(\Omega)^*. \tag{17}$$

Rotational invariance of the Hamiltonian implies that all rotated states distinguished by different orientations Ω,

$$|\Phi(\Omega)\rangle \equiv D(\Omega)|\Phi_0\rangle, \tag{18}$$

are degenerate. As $|\Phi(\Omega)\rangle$ represents a state with a definite spatial orientation Ω, it is independent of any other rotated state $|\Phi(\Omega')\rangle$ and the most general wavefunction corresponds to a superposition of the rotated states [11]

$$|\Psi\rangle = \int F(\Omega)\,|\Phi(\Omega)\rangle\, d\Omega = \int F(\Omega)\, D(\Omega)\,|\Phi_0\rangle\, d\Omega, \tag{19}$$

where $F(\Omega)$ is a weight function discussed further below. Equation (19) is a particular implementation of the *generator coordinate method* in which the Euler angles Ω acting as the generator coordinates.

2. Projection of Good Angular Momentum

Expanding the weight function $F(\Omega)$ as

$$F(\Omega) = \sum_{JMK} \frac{2J+1}{8\pi^2} F^J_{MK} D^J_{MK}(\Omega) \tag{20}$$

and inserting into Eq. (19) gives

$$|\Psi\rangle = \sum_{JMK} F^J_{MK} \hat{P}^J_{MK} |\Phi_0\rangle, \tag{21}$$

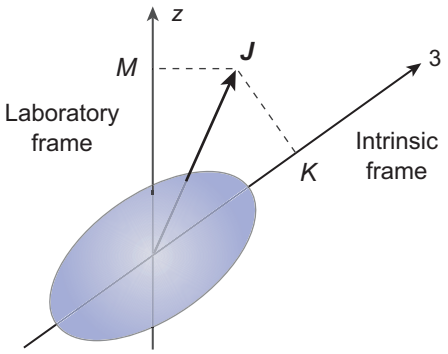

FIG. 5: Intrinsic and laboratory frames for a deformed nucleus of angular momentum J. The projection of J is M on the laboratory z-axis and K on the intrinsic 3-axis.

where $\hat{P}^J_{MK}$ has been defined by

$$\hat{P}^J_{MK} \equiv \frac{2J+1}{8\pi^2}\int D^J_{MK}(\Omega)D(\Omega)d\Omega. \tag{22}$$

The coefficients F^J_{MK} in Eq. (21) [this document] are now variational parameters that replace the weight function $F(\Omega)$ in Eq. (19) [this document]. Using Eqs. (15), (22) [this document], and the orthogonality of the D-functions (16) [this document], we find that the action of $\hat{P}^J_{MK}$ on a state of good angular momentum $|\nu J'K'\rangle$ (where ν denotes any additional quantum numbers that are required) is

$$\hat{P}^J_{MK}|\nu J'K'\rangle = \delta_{JJ'}\delta_{KK'}|\nu JM\rangle. \tag{23}$$

Thus $\hat{P}^J_{MK}$ is an *angular momentum projection operator* and $|\Phi\rangle$ in Eq. (21) [this document] is a state with indefinite angular momentum but the projected component $\hat{P}^J_{MK}|\Phi\rangle$ is a state of good angular momentum. The spectral representation of the projection operator is

$$\hat{P}^J_{MK} = \sum_{\nu}|\nu JM\rangle\langle\nu JK| \qquad \sum_{JM}\hat{P}^J_{MM} = 1, \tag{24}$$

which implies the projection properties

$$\left(\hat{P}^J_{MK}\right)^{\dagger} = \hat{P}^J_{KM} \qquad \hat{P}^J_{KM}\hat{P}^{J'}_{M'K'} = \delta_{JJ'}\delta_{MM'}\hat{P}^J_{KK'}. \tag{25}$$

If $|\Psi\rangle$ defined in Eq. (21) [this document] is viewed as a *trial variational state*, Eqs. (14) and (25) [this document] imply that the summation over J and M drops out and it is sufficient to carry out the variational calculation using the trial wavefunction

$$|\Psi\rangle = \sum_K F^J_K \hat{P}^J_{MK}|\Phi\rangle. \tag{26}$$

Therefore $|\Psi\rangle$ *is an eigenstate of angular momentum* (J,M).

Rotational invariance restored: The intrinsic state $|\Phi_0\rangle$ represents an entire band of rotational states but the variational wavefunction $|\Psi\rangle$ projects from $|\Phi_0\rangle$ a single rotationally invariant state of good angular momentum (J,M).

The rotational symmetry that was broken spontaneously by the deformed intrinsic state $|\Phi_0\rangle$ has been restored by projecting from the intrinsic state (representing a mixture of angular momenta) a state $|\Psi\rangle$ that has a single definite angular momentum.

B. Angular Momentum Content of an Intrinsic State

From the preceding discussion, the intrinsic state must contain within it all the angular momentum states that can be projected to give a rotational band. In general, states of definite angular momentum $|JMK\rangle$ can be written

$$|JMK\rangle = \hat{P}^J_{MK}|\Phi_0\rangle \tag{27}$$

where $\hat{P}^J_{MK}$ is the angular momentum projector defined in Eq. (22) [this document]. Then the the angular momentum content of the intrinsic state $|\Phi_0\rangle$ is a superpositiion of angular momenta [12]

$$|\Phi_0\rangle = \sum_{JM} C_{JM}|JM\rangle, \tag{28}$$

and the probability β_J that a state with eigenvalue $J(J+1)$ contributes to the intrinsic state $|\Phi_0\rangle$ is given by

$$\beta_J \equiv \sum_M |C_{JM}|^2 = \sum_M \langle\Phi_0|\hat{P}^J_{MM}|\Phi_0\rangle. \tag{29}$$

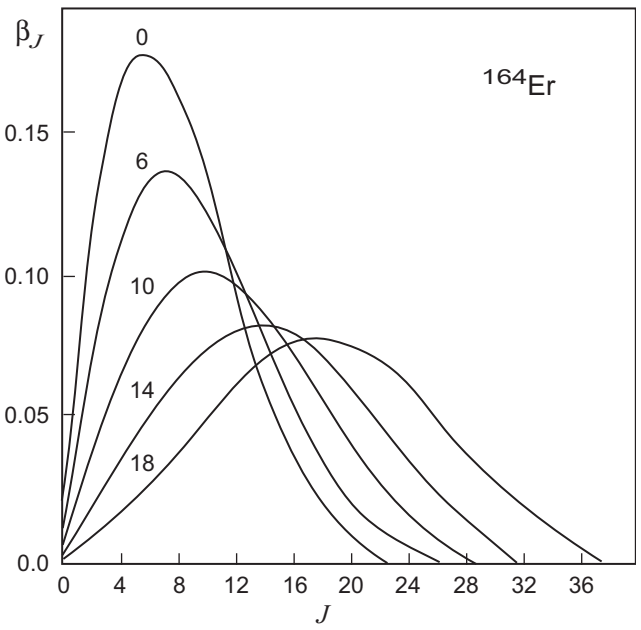

FIG. 6: Angular momentum content of intrinsic states from a self-consistent cranking model calculation for the nucleus ^{164}Er [12]. Curves are labeled by the expectation value of the angular momentum $\langle J_x\rangle = \sqrt{J(J+1)}$ for the state calculated in the cranking model. The vertical axis is the weight β_J defined in Eq. (29) [this document] and the horizontal axis gives the angular momentum components contributing to the state labeled by J.

Figure 6 [this document] illustrates the angular momentum content of an intrinsic state calculated in self-consistent cranking approximation for ^{164}Er (which has a highly deformed intrinsic state) [12]. A broad range of angular momenta contribute to each physical angular momentum, and only at the highest angular momenta do the peaks of curves coincide approximately with the actual angular momentum of the state.

For example, the ground state curve labeled by $\langle J_x\rangle = 0$ has only a small component of $J = 0$, its largest contributions come from angular momentum components with $J \sim 4-6\hbar$, and it contains non-trivial components of angular momenta all the way up to $J \sim 20\hbar$. The spread in angular momenta contributing to a state implies a spread in orientation angle of $\Delta\theta \sim 10$ degrees, by uncertainty principle arguments [12]. So such an intrinsic state contains a broad range of angular momentum components but has a relatively small range in orientation angle for the deformed state. This is reminiscent of *Wannier* states in condensed matter, where a superposition of spatially delocalized momentum-space wavefunctions produces a state that is spatially localized (see Section VI [this document]).

VI. INTRINSIC NUCLEAR STATES AND BLOCH'S THEOREM

This Section discusses the relationship between Bloch's theorem, which arises in condensed matter because of translational invariance, and projection of angular momentum wavefunctions from an intrinsic state, which arises in nuclear physics because of rotational invariance. This parallel is useful in constructing topological nuclear states, since the topological problem has been developed extensively in the condensed matter case.

A. Projection of Nuclear Angular Momentum

From Section V [this document], a general nuclear rotational wavefunction may be parameterized by Euler angles $\mathbf{\Omega} = (\alpha,\beta,\gamma)$ and takes the form

$$|\Phi(\mathbf{\Omega})\rangle = D(\mathbf{\Omega})|\Phi_0\rangle, \tag{30}$$

where $|\Phi_0\rangle$ is a deformed intrinsic wavefunction (see Fig. 5) [this document] that does not conserve angular momentum, so by uncertainty principle arguments it has a sharp orientation angle that we assume initially to be $\mathbf{\Omega}_0 = (0,0,0)$, the operator $D(\mathbf{\Omega})$ rotates an intrinsic wavefunction through an angle $\mathbf{\Omega}$ and is given by,

$$D(\mathbf{\Omega}) = e^{-i\alpha J_z}e^{-i\beta J_y}e^{-i\gamma J_z} = e^{-i\boldsymbol{J}\cdot\mathbf{\Omega}}, \tag{31}$$

and the $\boldsymbol{J} = (J_x,J_y,J_z)$ are angular momentum operators. Thus, the Hilbert space may be parameterized by the angles $\mathbf{\Omega}$ and the intrinsic wavefunction describing states in that space may be written

$$|\Phi(\mathbf{\Omega})\rangle = D(\mathbf{\Omega})|\Phi_0\rangle = e^{-i\boldsymbol{J}\cdot\mathbf{\Omega}}|\Phi_0\rangle, \tag{32}$$

where the angular coordinates $\mathbf{\Omega}$ of the Hilbert space impose periodic conditions on the wavefunctions, just as momentum periodicity of a crystal imposes periodic conditions on the wavefunctions of the Brillouin zone in condensed matter.

From Eqs. (26), (22), (19), and (20) [this document], a rotational wavefunction with good angular momentum $|JM\rangle$ can be expressed in the form

$$|JM\rangle = \sum_K f_{JK}\int d\mathbf{\Omega}\, D^J_{MK}(\mathbf{\Omega})\, D(\mathbf{\Omega})|\Phi_0\rangle, \tag{33}$$

where $f_{JK} \equiv (2J+1)F^J_K/8\pi^2$ with F^J_K the expansion coefficient in Eq. (26), the rotation operator $D(\mathbf{\Omega})$ is given explicitly by $D(\mathbf{\Omega}) = e^{i\boldsymbol{J}\cdot\mathbf{\Omega}}$, and $D^J_{MK}(\mathbf{\Omega})$ is the matrix element of the rotation operator in an angular momentum basis $|JMK\rangle$. The factors in the integrand of this equation have the following interpretation,

- $|\Phi_0\rangle$ is an intrinsic state with respect to rotational symmetry (fixed orientation angle; indeterminate angular momentum by the uncertainty principle, as illustrated in Fig. 6) [this document] with orientation angle $\mathbf{\Omega}_0 = (0,0,0)$;
- $D(\mathbf{\Omega})|\Phi_0\rangle$ is an intrinsic state with orientation angle $\mathbf{\Omega}$, where values of $\mathbf{\Omega}$ parameterize the Hilbert space;
- $D^J_{MK}(\mathbf{\Omega})$ is the matrix element of the rotation operator in a basis $|JMK\rangle$ of states having good angular momentum,

$$D^J_{MK}(\mathbf{\Omega}) = \langle JMK|D(\mathbf{\Omega})|JMK\rangle \tag{34}$$

with J the total angular momentum, M the projection of J on the laboratory z-axis, and K the projection of J on the intrinsic 3-axis (see Fig. 5) [this document].

Thus we wish to consider the topology of the rotated nuclear intrinsic states $D(\mathbf{\Omega})|\Phi_0\rangle$ on a Hilbert space parameterized by the angles $\mathbf{\Omega}$. Because of the periodicity of the angles, the Hilbert space may be expected to be toroidal and thus closed.

B. Bloch States in Condensed Matter

An electronic wavefunction for a periodic crystal is expected to take the form

$$\psi_{\boldsymbol{k}}(\boldsymbol{r}) = u_{\boldsymbol{k}}(\boldsymbol{r})e^{i\boldsymbol{k}\cdot\boldsymbol{r}} \qquad u_{\boldsymbol{k}}(\boldsymbol{r}) = u_{\boldsymbol{k}}(\boldsymbol{r}+\boldsymbol{T}), \tag{35}$$

where $\boldsymbol{T}$ is a lattice vector. This exemplifies *Bloch's theorem.*

> ***Bloch's theorem:*** Because of translational invariance, wavefunctions on a periodic lattice take the form (35) [this document] of a plane wave $e^{i\boldsymbol{k}\cdot\boldsymbol{r}}$ modulated by a function $u_{\boldsymbol{k}}(\boldsymbol{r})$ having the periodicity of the lattice.

The wavefunction (35) [this document] implied by Bloch's theorem is illustrated schematically in Fig. 7 [this document].

Bloch's theorem is of broad applicability because it derives solely from translational invariance.

It is most common in condensed matter to work in a momentum representation as for Eq. (35) [this document]. An alternative description of electronic structure may be given in terms of *Wannier functions*, which are electronic wavefunctions localized in real space that are Fourier transforms of the Bloch waves (35) [this document] in momentum space. Let's define the Wannier function $|W_0(\boldsymbol{r})\rangle$ for a unit cell located at coordinate $\boldsymbol{r}$ of the direct lattice by superposing every Bloch wave function $|\psi_{n\boldsymbol{k}}(\boldsymbol{r})\rangle$ of Eq. (35) [this document] with a $\boldsymbol{k}$ lying in the corresponding Brillouin zone (BZ) of the reciprocal lattice

$$|W_0(\boldsymbol{r})\rangle = \sum_{\boldsymbol{k}\in \mathrm{BZ}} |\psi_{n\boldsymbol{k}}(\boldsymbol{r})\rangle \simeq \frac{V}{(2\pi)^3}\int_{\mathrm{BZ}} |\psi_{n\boldsymbol{k}}(\boldsymbol{r})\rangle d\boldsymbol{k}, \qquad (36)$$

where n is a band index and V is the volume of a unit cell of the direct lattice. The Wannier functions in different unit cells of the direct lattice are related by translational invariance so the Wannier function $|W_0(\boldsymbol{r})\rangle$ can be translated a distance $\boldsymbol{R}$ by the translation operator $T(\boldsymbol{R}) = e^{-i\boldsymbol{k}\cdot\boldsymbol{R}}$ and we define

$$\begin{aligned} |W_{n\boldsymbol{R}}(\boldsymbol{r})\rangle &= \sum_{\boldsymbol{k}\in \mathrm{BZ}} T(\boldsymbol{R})|\psi_{n\boldsymbol{k}}(\boldsymbol{r})\rangle = \sum_{\boldsymbol{k}\in \mathrm{BZ}} e^{-i\boldsymbol{k}\cdot\boldsymbol{R}}|\psi_{n\boldsymbol{k}}(\boldsymbol{r})\rangle \\ &\simeq \frac{V}{(2\pi)^3}\int_{\mathrm{BZ}} e^{-i\boldsymbol{k}\cdot\boldsymbol{R}}\,|\psi_{n\boldsymbol{k}}(\boldsymbol{r})\rangle\, d\mathrm{k}, \end{aligned} \qquad (37)$$

The Wannier function $|W_{n\boldsymbol{R}}(\boldsymbol{r})\rangle$ in this equation has the form of a Fourier transform, so the inverse transform gives the Bloch wavefunction in momentum space

$$|\psi_{n\boldsymbol{k}}(\boldsymbol{r})\rangle = \sum_{\boldsymbol{R}} e^{i\boldsymbol{k}\cdot\boldsymbol{R}}\,|W_{n\boldsymbol{R}}(\boldsymbol{r})\rangle. \qquad (38)$$

Thus, Eqs. (37) and (38) [this document] transform between the momentum space and real space forms of the wavefunction. The Bloch functions $|\psi_{n\boldsymbol{k}}\rangle$ form an orthonormal set, as do the Wannier functions $|W_{n\boldsymbol{R}}\rangle$,

$$\langle\psi_{n\boldsymbol{k}}|\,\psi_{m\boldsymbol{k}'}\rangle = \frac{(2\pi)^3}{V}\,\delta_{nm}\delta_{\boldsymbol{k}\boldsymbol{k}'}, \qquad (39a)$$

$$\langle W_{n\boldsymbol{R}}|\,W_{m\boldsymbol{R}'}\rangle = \delta_{nm}\delta_{\boldsymbol{R}\boldsymbol{R}'}. \qquad (39b)$$

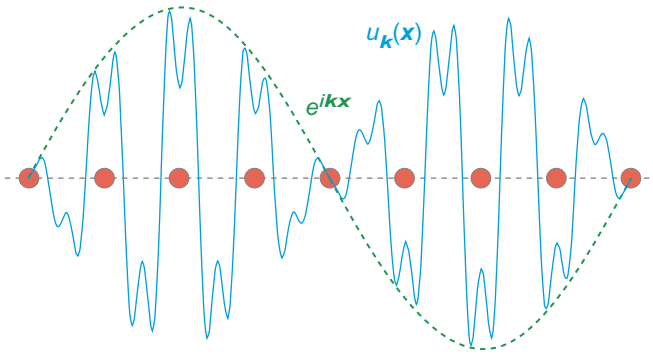

FIG. 7: The real part of a 1D Bloch wavefunction $\psi_{\boldsymbol{k}} = e^{i\boldsymbol{k}\cdot\boldsymbol{x}}u_{\boldsymbol{k}}(\boldsymbol{x})$ given by Eq. (35) [this document]. Circles represent the position of atoms. The dashed curve represents the plane wave $e^{i\boldsymbol{k}\cdot\boldsymbol{x}}$ and the solid curve is the function $u_{\boldsymbol{k}}(\boldsymbol{x})$ representing the effect of local atomic interaction with the electrons.

By uncertainty principle arguments the Bloch wavefunctions of Eq. (35) [this document] have definite momentum but uncertain position, while the Wannier wavefunctions of Eq. (37) [this document] have localized position but indefinite momentum. We may form a trial wavefunction by a superposition of Wannier functions,

$$\begin{aligned} |\psi\rangle &= \int d\boldsymbol{R}\, f(\boldsymbol{R}) W_{n\boldsymbol{r}}(\boldsymbol{r}) \\ &= \int d\boldsymbol{R}\, f(\boldsymbol{R}) \sum_{\boldsymbol{k}\in \mathrm{BZ}} e^{i\boldsymbol{k}\cdot\boldsymbol{r}} T(\boldsymbol{R})|u_{\boldsymbol{k}}(\boldsymbol{r})\rangle \\ &= \sum_{\boldsymbol{k}\in \mathrm{BZ}} \int d\boldsymbol{R}\, f(\boldsymbol{R}) e^{i\boldsymbol{k}\cdot\boldsymbol{r}}\, T(\boldsymbol{R})\,|u_{\boldsymbol{k}}(\boldsymbol{r})\rangle, \end{aligned} \qquad (40)$$

where $f(\boldsymbol{R})$ is a weight function, Eq. (35) [this document] was used, $e^{i\boldsymbol{k}\cdot\boldsymbol{r}}$ is a translational eigenfunction, $T(\boldsymbol{R}) = e^{-i\boldsymbol{k}\cdot\boldsymbol{R}}$ is the translation operator, and $|u_{\boldsymbol{k}}(\boldsymbol{r})\rangle$ may be interpreted as an intrinsic state.

The states $|\psi\rangle$ of Eq. (40) [this document] are not states of good momentum because of the sum over $\boldsymbol{k}$, but if we followed a similar procedure as in Eqs. (19)-(26) [this document] for the rotational case and expanded the weight factor $f(\boldsymbol{R})$ in states of good linear momentum we could presumably introduce a projector for linear momentum and eliminate the sum over $\boldsymbol{k}$. If we ignore the weight $f(\boldsymbol{R})$ and the sum over $\boldsymbol{k}$ in Eq. (40) [this document], we may interpret the factors in the integrand as follows.

- $|u_{\boldsymbol{k}}(\boldsymbol{r})\rangle$ is an intrinsic state with respect to translational symmetry, with position $\boldsymbol{r}$.
- $T(\boldsymbol{R})\,|u_{\boldsymbol{k}}(\boldsymbol{r})\rangle = e^{-i\boldsymbol{k}\cdot\boldsymbol{R}}|u_{\boldsymbol{k}}(\boldsymbol{r})\rangle$ is an intrinsic state with respect to translational symmetry having position $\boldsymbol{r}-\boldsymbol{R}$, where values of $\boldsymbol{r}-\boldsymbol{R}$ parameterize the Hilbert space. The periodicity implied by Bloch's theorem means that the coordinates parameterizing Hilbert space will become angles parameterizing a torus.
- $e^{i\boldsymbol{k}\cdot\boldsymbol{r}}$ is a translational eigenfunction in a basis of good linear momentum.

These are seen to parallel the interpretation of the factors in the integrand of Eq. (33) [this document] given in Section VI A [this document].

C. Comparison of Bloch and Nuclear States

Comparing Eqs. (33) and (40) [this document], we see that a Bloch wave (35) [this document]in a crystal has a very similar structure to the nuclear rotational wavefunction (32) [this document], with translational invariance being central to Eq. (35) [this document] and rotational invariance being central to Eq. (32) [this document], and with $u_{\boldsymbol{k}}(\boldsymbol{r})$ playing a similar role in the Bloch wave as the intrinsic state $|\Phi_0\rangle$ plays for the rotational state.

1. For the nuclear wavefunction the intrinsic rotational state $|\Phi_0\rangle$ has a fixed orientation angle [chosen to be

$\boldsymbol{\Omega} = (0,0,0)$] and by the uncertainty principle it violates conservation of angular momentum maximally. From Eq. (36) [this document], for the Wannier wavefunction localized at position $\boldsymbol{r}$ of a unit cell on the direct lattice,

$$|W_0(\boldsymbol{r})\rangle = \sum_{\boldsymbol{k}\in \mathrm{BZ}} |\psi_{n\boldsymbol{k}}(\boldsymbol{r})\rangle = \sum_{\boldsymbol{k}\in \mathrm{BZ}} e^{i\boldsymbol{k}\cdot\boldsymbol{r}} |u_{\boldsymbol{k}}(\boldsymbol{r})\rangle,$$

where Eq. (35) [this document] was used. This suggests that the Wannier state $|W_0(\boldsymbol{r})\rangle$ behaves as an *intrinsic state* analogous to the nuclear intrinsic state $|\Phi_0\rangle$.

- The nuclear intrinsic state $|\Phi_0\rangle$ violates rotational symmetry because of its fixed orientation angle $\boldsymbol{\Omega}_0 = (0,0,0)$;
- the Wannier intrinsic state $|W_0(\boldsymbol{r})\rangle$ violates translational symmetry because of its localized position $\boldsymbol{r}$.

2. In the nuclear case the intrinsic rotational state at orientation angle $\boldsymbol{\Omega}$,

$$\Phi(\boldsymbol{\Omega}) = D(\boldsymbol{\Omega})|\Phi_0\rangle = e^{i\boldsymbol{J}\cdot\boldsymbol{\Omega}}|\Phi_0\rangle,$$

where $D(\boldsymbol{\Omega})$ is the operator rotating through an angle $\boldsymbol{\Omega}$, is also an intrinsic state that violates rotational symmetry because it has a definite orientation angle $\boldsymbol{\Omega}$. Likewise, the translated Wannier state at location $\boldsymbol{r}-\boldsymbol{R}$,

$$\begin{aligned} |W_{n\boldsymbol{R}}(\boldsymbol{r})\rangle &= \frac{V}{(2\pi)^3}\int_{\mathrm{BZ}} |\psi_{n\boldsymbol{k}}(\boldsymbol{r})\rangle\, e^{-i\boldsymbol{k}\cdot\boldsymbol{R}}\, d\boldsymbol{k} \\ &= \frac{V}{(2\pi)^3}\int_{\mathrm{BZ}} e^{-i\boldsymbol{k}\cdot(\boldsymbol{r}-\boldsymbol{R})}\, |u_{n\boldsymbol{k}}(\boldsymbol{r})\rangle\, d\boldsymbol{k}, \end{aligned}$$

is an intrinsic state that violates translational symmetry because of its fixed location $\boldsymbol{r}-\boldsymbol{R}$.

3. In both nuclear and Wannier cases we can use the symmetry-breaking intrinsic states to convert to states of good angular momentum and linear momentum, respectively, by taking a superposition of intrinsic states having all possible angular momenta and linear momenta, respectively. For the nuclear case a state of good angular momentum (JM) is given by Eq. (33) [this document],

$$|JM\rangle = \sum_K f_{JK}\int d\boldsymbol{\Omega}\, D^J_{MK}(\boldsymbol{\Omega})\, D(\boldsymbol{\Omega})|\Phi_0\rangle.$$

For the condensed matter case, a corresponding state is given by Eq. (40),

$$|\psi\rangle = \sum_{\boldsymbol{k}\in \mathrm{BZ}}\int d\boldsymbol{R}\, f(\boldsymbol{R}) e^{i\boldsymbol{k}\cdot\boldsymbol{r}}\, T(\boldsymbol{R})\, |u_{\boldsymbol{k}}(\boldsymbol{r})\rangle.$$

Thus, with respect to evaluation of Berry phases and Berry curvature in the nuclear Hilbert space, the intrinsic rotational states are the candidates for evaluation of matrix elements, just as the intrinsic states $|u_{\boldsymbol{k}}(\boldsymbol{r})\rangle$ are used in condensed matter to evaluate matrix elements to construct Berry phases and Berry curvature on the Hilbert space of states.

In this connection it is important to note the conclusion in condensed matter that one *must* use the "intrinsic state" $|u_{\boldsymbol{k}}\rangle$ (the "cell periodic wavefunction") to construct Berry phases and Berry curvatures rather than the full wavefunction $|\psi_{n_{\mathrm{k}}}\rangle$ appearing in Eq. (35) [this document]; see the comments in Section 3.4 of Vanderbilt [2]. Basically the argument is that all the $|u_{\boldsymbol{k}}\rangle$ belong to the same Hilbert space but that is not true of all the $|\psi_{n\boldsymbol{k}}\rangle$. The net effect is that using $|u_{\boldsymbol{k}}\rangle$ ensures finite and well behaved integrals. This, and the parallels between the condensed matter and nuclear cases discussed in this section, provide further encouragement that our proposal to use intrinsic rotational states for computing Berry phases and Berry curvature for the nuclear case is perhaps on the right track.

VII. SAMPLE CALCULATIONS

In this section some example calculations are shown to illustrate techniques likely to be important in evaluating possible nuclear topological states.

A. Single Electron in a Magnetic Field

This example illustrates calculating the Berry curvature and Berry phase for a single electron in a magnetic field. It is adapted from the solution of Prob. 27.6 in Ref. [9]. The Hamiltonian for an electron interacting with a magnetic field $\boldsymbol{B}$ may be written

$$\begin{aligned} H &= -\frac{1}{2}\mu\,\boldsymbol{\sigma}\cdot\boldsymbol{B} \\ &= -\frac{1}{2}\mu\left(\sigma_x B_x + \sigma_y B_y + \sigma_z B_z\right), \end{aligned} \tag{41}$$

where the σ_i are Pauli matrices,

$$\sigma_x = \begin{pmatrix} 0 & 1 \\ 1 & 0 \end{pmatrix} \qquad \sigma_y = \begin{pmatrix} 0 & -i \\ i & 0 \end{pmatrix} \qquad \sigma_z = \begin{pmatrix} 1 & 0 \\ 0 & -1 \end{pmatrix},$$

The eigenvalues for the Schrödinger equation $H|\psi\rangle = E|\psi\rangle$ are

$$E_\pm(B) = \pm\frac{1}{2}\mu\sqrt{B_x^2+B_y^2+B_z^2} = \pm\frac{1}{2}\mu B, \tag{42}$$

where $B \equiv |\boldsymbol{B}|$, and the corresponding eigenvectors are given by

$$|\psi_+\rangle = \begin{pmatrix} \cos\frac{\theta}{2}e^{-i\phi/2} \\ \sin\frac{\theta}{2}e^{i\phi/2} \end{pmatrix} \quad |\psi_-\rangle = \begin{pmatrix} -\sin\frac{\theta}{2}e^{-i\phi/2} \\ \cos\frac{\theta}{2}e^{i\phi/2} \end{pmatrix}, \tag{43}$$

where the angles θ and ϕ are related to the magnetic field components by

$$B_x = B\sin\theta\cos\phi \quad B_y = B\sin\theta\sin\phi \quad B_z = B\cos\theta.$$

The Berry phase may be expressed in the form (11), which requires evaluation of the quantity $\nabla_B H(\boldsymbol{B})$. For the Hamiltonian (41),

$$\begin{aligned}\nabla_B H(\boldsymbol{B}) &= \nabla_B\left(-\frac{\mu}{2}\boldsymbol{\sigma}\cdot\boldsymbol{B}\right)\\ &= -\frac{\mu}{2}\left(\boldsymbol{i}\frac{\partial}{\partial X}+\boldsymbol{j}\frac{\partial}{\partial Y}+\boldsymbol{k}\frac{\partial}{\partial Z}\right)(\sigma_x X+\sigma_y Y+\sigma_z Z)\\ &= -\frac{\mu}{2}(\boldsymbol{i}\sigma_x+\boldsymbol{j}\sigma_y+\boldsymbol{k}\sigma_z)\\ &= \frac{\mu}{2}\boldsymbol{\sigma}.\end{aligned}$$

The Berry curvature is given by Eq. (11) [this document]. Letting $m=|\psi_-\rangle$ and $n=|\psi_+\rangle$ in that expression, we must evaluate

$$\frac{\langle m\boldsymbol{B}|\nabla_{\boldsymbol{B}}H|n\boldsymbol{B}\rangle\times\langle n\boldsymbol{B}|\nabla_{\boldsymbol{B}}H|m\boldsymbol{B}\rangle}{(E_n(\boldsymbol{B})-E_n(\boldsymbol{B}))^2}=\frac{\langle\psi_-|\nabla_{\boldsymbol{B}}H|\psi_+\rangle\times\langle\psi_+|\nabla_{\boldsymbol{B}}H|\psi_-\rangle}{(E_--E_+)^2}=\frac{\frac{\mu^2}{4}\langle\psi_-|\boldsymbol{\sigma}|\psi_+\rangle\times\langle\psi_+|\boldsymbol{\sigma}|\psi_-\rangle}{(E_--E_+)^2}$$

$$=\frac{\mu^2}{4(E_--E_+)^2}\begin{vmatrix}\boldsymbol{i} & \boldsymbol{j} & \boldsymbol{k}\\ \langle-|\sigma_x|+\rangle & \langle-|\sigma_y|+\rangle & \langle-|\sigma_z|+\rangle\\ \langle+|\sigma_x|-\rangle & \langle+|\sigma_y|-\rangle & \langle+|\sigma_z|-\rangle\end{vmatrix}=\frac{\mu^2}{4(E_--E_+)^2}\begin{pmatrix}\langle-|\sigma_y|+\rangle\langle+|\sigma_z|-\rangle-\langle-|\sigma_z|+\rangle\langle+|\sigma_y|-\rangle\\ -\langle-|\sigma_x|+\rangle\langle+|\sigma_z|-\rangle+\langle-|\sigma_z|+\rangle\langle+|\sigma_x|-\rangle\\ \langle-|\sigma_x|+\rangle\langle+|\sigma_y|-\rangle-\langle-|\sigma_y|+\rangle\langle+|\sigma_x|-\rangle\end{pmatrix}.$$

To evaluate this expression, let us choose a coordinate system such that the z axis points in the direction of the magnetic field $\boldsymbol{B}$,

$$\sigma_z|\pm\rangle=\pm|\pm\rangle\qquad\sigma_x|\pm\rangle=|\mp\rangle\qquad\sigma_y|\pm\rangle=\pm|\mp\rangle.$$

Then, for example,

$$\begin{aligned}&\langle-|\sigma_x|+\rangle\langle+|\sigma_y|-\rangle-\langle-|\sigma_y|+\rangle\langle+|\sigma_x|-\rangle=\\ &\quad -i\langle-|-\rangle\langle+|+\rangle-i\langle-|-\rangle\langle+|+\rangle=-2i.\end{aligned}$$

Evaluating the other matrix elements in a similar way leads to the result

$$\langle m\boldsymbol{B}|\nabla_{\boldsymbol{B}}H|n\boldsymbol{B}\rangle\langle n\boldsymbol{B}|\nabla_{\boldsymbol{B}}H|m\boldsymbol{B}\rangle=\frac{\mu^2}{4}\begin{pmatrix}0\\0\\-2i\end{pmatrix}.$$

Then from Eq. (11) [this document],

$$\begin{aligned}\boldsymbol{\Omega}_-(\boldsymbol{B}) &= i\left(\frac{\langle-|\nabla_{\boldsymbol{B}}H|+\rangle\langle+|\nabla_{\boldsymbol{B}}H|-\rangle}{(E_--E_+)^2}\right)\\ &= i\left[\left(\frac{1}{\frac{\mu}{2}(-B-B)}\right)^2\left(\frac{\mu^2}{4}\right)\begin{pmatrix}0\\0\\-2i\end{pmatrix}\right]\\ &= i\left[\frac{1}{4B^2}\begin{pmatrix}0\\0\\-2i\end{pmatrix}\right]\\ &= -\frac{1}{2B^2}\begin{pmatrix}0\\0\\1\end{pmatrix}.\end{aligned}$$

This result was obtained assuming a unit vector in the z direction, which is of the form $\boldsymbol{B}/B$, so the general solution for arbitrary axes is

$$\boldsymbol{\Omega}_-(\boldsymbol{B})=-\frac{1}{2}\left(\frac{\boldsymbol{B}}{B^3}\right).$$

By a similar analysis,

$$\boldsymbol{\Omega}_+(\boldsymbol{B})=\frac{1}{2}\left(\frac{\boldsymbol{B}}{B^3}\right).$$

These are the results that would be expected for a magnetic monopole of strength $\pm\frac{1}{2}$ placed at the origin of parameter space.

B. Chern Numbers on a 2D Torus

This example illustrates calculating the Berry phase and Chern numbers for a band with states in a Hilbert space defined on a 2-torus, as displayed in Fig. 9(a) [this document]. It was adapted from the solution of Prob. 28.6 in Ref. [9] which is specifically for a 2D Brillouin zone. Here we work with a general Hilbert space defined in terms of two periodic angular coordinates. The Berry flux or Berry phase γ_n for a band labeled by an index n can be defined by the integral over the Hilbert space

$$\gamma_n=\int_S\Omega^n_{\theta\phi}dS, \tag{44}$$

with the *Berry curvature tensor* given by

$$\Omega^n_{\theta\phi}\equiv\partial_\theta A^n_\phi(\theta,\phi)-\partial_\phi A^n_\theta(\theta,\phi), \tag{45}$$

where we parameterize the Hilbert space in terms of angles (θ,ϕ) on the 2-torus of Fig. 8 [this document], and the Berry

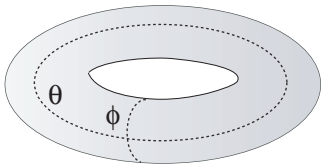

FIG. 8: Angular coordinates (θ,ϕ) for a 2-torus.

connections A_i are given by

$$A_\theta \equiv \langle\psi|i\partial_\theta|\psi\rangle \qquad A_\phi \equiv \langle\psi|i\partial_\phi|\psi\rangle, \tag{46}$$

where wavefunctions in the Hilbert space are denoted by $|\psi\rangle$ and we use the shorthand notation

$$\partial_\theta \equiv \frac{\partial}{\partial\theta} \qquad \partial_\phi \equiv \frac{\partial}{\partial\phi}.$$

From Eqs. (44) and (45) [this document], the Berry phase γ evaluated over the entire Hilbert space of wavefunctions is given by

$$\gamma_n \equiv \int_S \Omega^n_{\theta\phi} dS = \int_{\theta_\mathrm{i}}^{\theta_\mathrm{f}} d\theta \int_0^{2\pi} d\phi(\partial_\theta A_\phi - \partial_\phi A_\theta). \tag{47}$$

In general, states on the boundaries of the angular range are related by a phase (gauge) factor

$$|\psi_{n,\phi=2\pi}\rangle = e^{i\eta}|\psi_{n,\phi=0}\rangle \tag{48}$$

that we are free to choose (see the discussion in Vanderbilt [2], p. 46). Here we shall assume a *periodic gauge condition* by setting the phase factor to unity so that A_θ at $\phi=0$ and $\phi=2\pi$ are equivalent, even up to phases: $|\psi_{n,\phi=0}\rangle = |\psi_{n,\phi=2\pi}\rangle$. Thus the second term in the integral (47) [this document] vanishes because

$$\int_{\theta_\mathrm{i}}^{\theta_\mathrm{f}} d\theta \int_0^{2\pi} d\phi(\partial_\phi A_\theta) = \int_{\theta_\mathrm{i}}^{\theta_\mathrm{f}} d\theta \int_{A_\theta(0)}^{A_\theta(2\pi)} dA_\theta = 0, \tag{49}$$

since by the periodic gauge condition $A_\theta(2\pi) = A_\theta(0)$. Thus

$$\begin{aligned}\gamma_n &\equiv \int_S \Omega^n_{\theta\phi} dS = \int_{\theta_\mathrm{i}}^{\theta_\mathrm{f}} d\theta \int_0^{2\pi} d\phi \frac{\partial A_\phi}{\partial\theta} \\ &= \int_{\theta_\mathrm{i}}^{\theta_\mathrm{f}} d\theta \frac{\partial}{\partial\theta} \int_0^{2\pi} d\phi A_\phi = \int_{\theta_\mathrm{i}}^{\theta_\mathrm{f}} d\theta \frac{\partial\gamma^\phi}{\partial\theta} \\ &= \int_{\theta_\mathrm{i}}^{\theta_\mathrm{f}} d\gamma^\phi = \gamma^\phi(\theta_\mathrm{f}) - \gamma^\phi(\theta_\mathrm{i}),\end{aligned} \tag{50}$$

where in line 2 we have used that the Berry phase evaluated for a cyclic path in ϕ is

$$\gamma^\phi = \int_0^{2\pi} A_\phi d\phi,$$

from Eq. (44) [this document]. On the torus the endpoints for θ are identified modulo 2π, so at the end of a cycle in θ the Berry phase will have evolved by

$$\gamma = \gamma^\phi(\theta_\mathrm{f}) - \gamma^\phi(\theta_\mathrm{i}) = 2\pi m, \tag{51}$$

where m is an integer. But from the *Chern equation,*

$$\frac{1}{2\pi}\int_S \Omega\, dA = C, \tag{52}$$

where $C \equiv C_1$ is an integer *Chern number* (of the first type). Thus the Berry phase is related to the Chern number C by

$$\gamma \equiv \int_S \Omega_{\theta\phi} dS = 2\pi C. \tag{53}$$

Comparing Eqs. (51) and (50) [this document] gives $C=m$, and the Chern index may be interpreted as the winding number m along ϕ in one cycle over θ, as illustrated in Fig. 9(b-g) [this document]. For example, from Eq. (51) [this document] we have $\gamma^\phi(\theta_\mathrm{f}) - \gamma^\phi(\theta_\mathrm{i})$, so

1. if $m=0$, then as θ varies from 0 to 2π the phase ϕ varies from $\phi(\theta_\mathrm{i})$ to $\phi(\theta_\mathrm{i}+2\pi m) = \phi(\theta_\mathrm{i})$, as illustrated in Fig. 9(b) [this document]. The corresponding winding on the torus is illustrated in Fig. 9(e) [this document];

2. if $m=1$, then as θ varies from 0 to 2π the phase ϕ varies from $\phi(\theta_\mathrm{i})$ to $\phi(\theta_\mathrm{i}+2\pi m) = \phi(\theta_\mathrm{i}+2\pi)$, as illustrated in Fig. 9(c) [this document]. The corresponding winding on the torus is illustrated in Fig. 9(f) [this document];

3. if $m=2$, then as θ varies from 0 to 2π the phase ϕ varies from $\phi(\theta_\mathrm{i})$ to $\phi(\theta_\mathrm{i}+2\pi m) = \phi(\theta_\mathrm{i}+4\pi)$, as illustrated in Fig. 9(d) [this document]. The corresponding winding on the torus is illustrated in Fig. 9(g) [this document].

Thus, the integral Chern numbers may be interpreted as winding numbers on the 2-torus of Fig. 9(a) [this document].

VIII. VISUALIZING THE 2D-ROTOR HILBERT SPACE

We may visualize the topology of the 2D-rotor Hilbert space if the angular variable β with range $0-\pi$ is mapped to a variable $\beta' \equiv 2\beta$ with range $0-2\pi$. Then, identifying $\gamma=0$ with $\gamma=2\pi$, and $\beta'=0$ with $\beta'=2\pi$, the Hilbert space is topologically the 2-torus in Fig. 9(a) [this document]. The phase $\phi(\gamma)$ must return to its initial value for once around the torus in the γ direction, but only modulo an integer multiple of 2π:

$$\phi(\gamma=2\pi) = \phi(\gamma=0) + 2\pi m = \phi(\gamma=0) + 2\pi C_1. \tag{54}$$

This implies that the Chern number C_1 may be interpreted as a winding number m giving the number of times the torus is wrapped in the β' direction as γ is varied once around the torus, as illustrated in Fig. 9(b-g) [this document]. Three examples for the variation of $\phi(\gamma)$ are illustrated in Fig. 9 [this document].

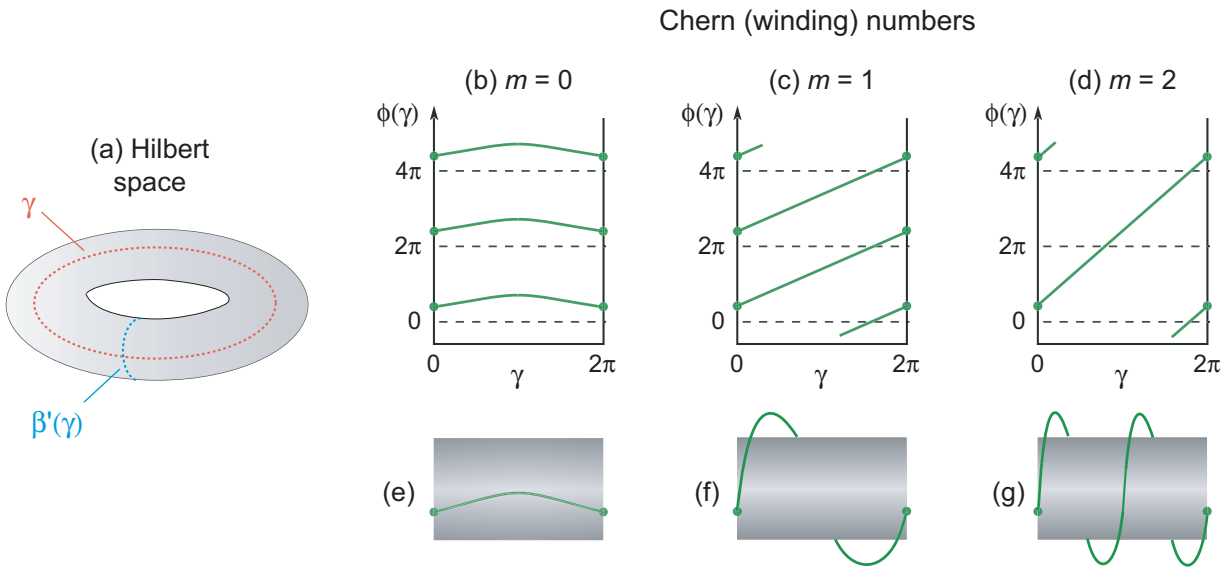

FIG. 9: Chern numbers C_1 associated with the 2D quantum rotor Hilbert space, for angular variables $(\beta' = 2\beta, \gamma)$. (a) The toroidal Hilbert space parameterized by the periodic angular variables γ and $\beta'(\gamma)$, with the cyclic coordinate $\beta' \equiv 2\beta$ assumed to range 0 to 2π. (b-g) Winding numbers corresponding to Chern numbers $C_1 = m = 0, 1, 2, \ldots$, with $\phi(\gamma = 2\pi) = \phi(\gamma = 0) + 2\pi m$. The points $\gamma = 0$ and $\gamma = 2\pi$ are assumed to be identified, so each cylinder in (e-g) is actually the closed 2-torus in (a). On the 2-torus the winding numbers then define distinct topological sectors of the theory labeled by $C_1 = m = 0, 1, 2, \ldots$, and a solution in one sector cannot be deformed continuously into one in another sector.

1. In Fig. 9(b, e) [this document], $C_1 = 0$ and the phase $\phi(\gamma)$ varies from $\phi(0)$ at $\gamma = 0$ to $\phi(0)$ at $\gamma = 2\pi$. The corresponding winding number is $m = C_1 = 0$, as illustrated in Fig. 9(e) [this document], which lies in the trivial topological sector where standard nuclear structure is formulated.

2. In Fig. 9(c, f) [this document], $C_1 = 1$ and the phase $\phi(\gamma)$ varies from $\phi(0)$ at $\gamma = 0$ to $\phi(0) + 2\pi$ at $\gamma = 2\pi$. The corresponding winding number is $m = C_1 = 1$, as illustrated in Fig. 9(f) [this document]: $\phi(\gamma)$ wraps once around the torus of Fig. 9(a) [this document]in the β' direction as γ varies from 0 to 2π.

3. In Fig. 9(d, g) [this document], $C_1 = 2$ and the phase $\phi(\gamma)$ varies from $\phi(0)$ at $\gamma = 0$ to $\phi(0) + 4\pi$ at $\gamma = 2\pi$. The corresponding winding number is $m = C_1 = 2$, as illustrated in Fig. 9(g) [this document]: $\phi(\gamma)$ wraps twice around the torus of Fig. 9(a) [this document] in the β' direction as γ varies from 0 to 2π.

Clearly the three solutions labeled by $m = C_1 = \{0, 1, 2\}$ in Fig. 9 [this document] cannot be deformed continuously into each other since the winding is around a torus; hence, they are topologically distinct and the corresponding values of the integers $m = C_1$ are *topologically protected invariants*.

IX. CHERN THEOREM FOR 2D ROTOR HILBERT SPACE

This section contains derivations and technical details associated with Chern quantization of a quantum rotor with 2D Hilbert space.

A. Angular Momentum Operators

The orientation angles for the rotor restricted to two orientation angles can also be expressed in the standard spherical coordinate system (θ, ϕ) illustrated in Fig. 1(c). Comparing the Euler angles (β, γ) in Fig. 1(b) with the spherical polar angles (θ, ϕ) in Fig. 1(c), successive rotations through the Euler angles γ and then β, and successive rotations through the polar angles ϕ and then θ, are related by

$$e^{i\beta\hat{J}_y} e^{i\gamma\hat{J}_z} \leftrightarrow e^{i\theta\hat{J}_y} e^{i\phi\hat{J}_z}.$$

Therefore, the 2D Euler-angle coordinate system in Fig. 1(b) is equivalent to the spherical polar coordinate system in Fig. 1(c) under the mapping $\theta \leftrightarrow \beta$. and $\phi \leftrightarrow \gamma$, and this mapping may be used to express formulas valid for the spherical polar coordinates (θ, ϕ) in the 2D Euler-angle space (β, γ). For example, the coordinate representation of the angular momentum operators

(J_x, J_y, J_z) in the (β, γ) coordinates is obtained from standard formulas expressed in spherical coordinates using the mapping $(\theta, \phi) \leftrightarrow (\beta, \gamma)$ as

$$\hat{J}_x = i\hbar \left(\sin\gamma \frac{\partial}{\partial \beta} + \cot\beta \cos\gamma \frac{\partial}{\partial \gamma} \right), \tag{55a}$$

$$\hat{J}_y = i\hbar \left(-\cos\gamma \frac{\partial}{\partial \beta} + \cot\beta \cos\gamma \frac{\partial}{\partial \gamma} \right), \tag{55b}$$

$$\hat{J}_z = -i\hbar \frac{\partial}{\partial \gamma}. \tag{55c}$$

(We may drop the explicit factors of $\hbar$ if $\hbar = 1$ units are chosen.)

Let's find expectation values of angular momentum components for the lab frame $(\hat{J}_x, \hat{J}_y, \hat{J}_z)$ and the intrinsic frame $(\hat{J}_1, \hat{J}_2, \hat{J}_3)$. Consider $\hat{J}_x$ in the lab frame; utilizing Eq. (8),

$$\langle \psi | \hat{J}_x | \psi \rangle = \langle \Phi | e^{i\gamma \hat{J}_z} e^{i\beta \hat{J}_y} \hat{J}_x e^{-i\beta \hat{J}_y} e^{-i\gamma \hat{J}_z} | \Phi \rangle. \tag{56}$$

But if the intrinsic-frame operator component $\hat{J}_1$ is defined in terms of the lab-frame component $\hat{J}_x$ by

$$\hat{J}_1 = \hat{D}^{-1} \hat{J}_x \hat{D} = e^{i\gamma \hat{J}_z} e^{i\beta \hat{J}_y} \hat{J}_x e^{-i\beta \hat{J}_y} e^{-i\gamma \hat{J}_z}, \tag{57}$$

then $\langle \psi | \hat{J}_x | \psi \rangle = \langle \Phi | \hat{J}_1 | \Phi \rangle$. and from Eqs. (56)-(57) [this document],

$$\langle \psi | \hat{J}_x | \psi \rangle = \langle \Phi | e^{i\gamma \hat{J}_z} e^{i\beta \hat{J}_y} \hat{J}_x e^{-i\beta \hat{J}_y} e^{-i\gamma \hat{J}_z} | \Phi \rangle = \langle \Phi | \hat{J}_1 | \Phi \rangle, \tag{58}$$

where $\hat{J}_x$ and $|\psi\rangle$ are lab-frame and $\hat{J}_1$ and $|\Phi\rangle$ are intrinsic-frame quantities. Now consider $\hat{J}_y$ in the lab frame,

$$\begin{aligned} \langle \psi | \hat{J}_y | \psi \rangle &= \langle \Phi | e^{i\gamma \hat{J}_z} e^{i\beta \hat{J}_y} \hat{J}_y e^{-i\beta \hat{J}_y} e^{-i\gamma \hat{J}_z} | \Phi \rangle \\ &= \langle \Phi | e^{i\gamma \hat{J}_z} e^{i\beta \hat{J}_y} e^{-i\beta \hat{J}_y} \hat{J}_y e^{-i\gamma \hat{J}_z} | \Phi \rangle \\ &= \langle \Phi | e^{i\gamma \hat{J}_z} \hat{J}_y e^{-i\gamma \hat{J}_z} | \Phi \rangle, \end{aligned} \tag{59}$$

where we have used that $[A, e^B] = 0$ only if $[A, B] = 0$. But defining the intrinsic frame operator component $\hat{J}_2 \equiv \hat{D}^{-1} \hat{J}_y \hat{D}$ in terms of the lab frame component $\hat{J}_y$,

$$\hat{J}_2 \equiv e^{i\gamma \hat{J}_z} e^{i\beta \hat{J}_y} \hat{J}_y e^{-i\beta \hat{J}_y} e^{-i\gamma \hat{J}_z} = e^{i\gamma \hat{J}_z} \hat{J}_y e^{-i\gamma \hat{J}_z}, \tag{60}$$

and using $\langle \psi | \hat{J}_y | \psi \rangle = \langle \Phi | \hat{J}_2 | \Phi \rangle$ and Eq. (59) [this document],

$$\langle \psi | \hat{J}_y | \psi \rangle = \langle \Phi | e^{i\gamma \hat{J}_z} \hat{J}_y e^{-i\gamma \hat{J}_z} | \Phi \rangle = \langle \Phi | \hat{J}_2 | \Phi \rangle, \tag{61}$$

where $\hat{J}_y$ and $|\psi\rangle$ are defined in the lab frame, and $\hat{J}_2$ and $|\Phi\rangle$ are defined in the intrinsic frame. Finally, consider the expectation value of $\hat{J}_z$ evaluated in the laboratory frame,

$$\langle \psi | \hat{J}_z | \psi \rangle = \langle \Phi | e^{i\gamma \hat{J}_z} e^{i\beta \hat{J}_y} \hat{J}_z e^{-i\beta \hat{J}_y} e^{-i\gamma \hat{J}_z} | \Phi \rangle. \tag{62}$$

If the intrinsic-frame operator component $\hat{J}_3$ is defined by

$$\hat{J}_3 \equiv \hat{D}^{-1} \hat{J}_z \hat{D} = e^{i\gamma \hat{J}_z} e^{i\beta \hat{J}_y} \hat{J}_z e^{-i\beta \hat{J}_y} e^{-i\gamma \hat{J}_z}, \tag{63}$$

then $\langle \psi | \hat{J}_z | \psi \rangle = \langle \Phi | \hat{J}_3 | \Phi \rangle$ and from Eqs. (62)-(63) [this document],

$$\langle \psi | \hat{J}_z | \psi \rangle = \langle \Phi | e^{i\gamma \hat{J}_z} e^{i\beta \hat{J}_y} \hat{J}_z e^{-i\beta \hat{J}_y} e^{-i\gamma \hat{J}_z} | \Phi \rangle = \langle \Phi | \hat{J}_3 | \Phi \rangle, \tag{64}$$

with $\hat{J}_z$ and $|\psi\rangle$ laboratory and $\hat{J}_3$ and $|\Phi\rangle$ intrinsic quantities.

B. Important Commutation Relations

In the derivations in this paper it will often be necessary to commute operators in expressions. In doing so we will use extensively that an operator $\hat{A}$ commutes with a function $f(\hat{A})$ of that operator

$$[\hat{A}, f(\hat{A})] = 0. \tag{65}$$

For example, Eq. (55c) [this document] implies that $e^{-i\gamma\hat{J}_z}$ is a function of the derivative operator $\frac{\partial}{\partial\gamma}$,

$$e^{-i\gamma\hat{J}_z} = e^{-\gamma\frac{\partial}{\partial\gamma}} = f(\tfrac{\partial}{\partial\gamma}), \tag{66}$$

and therefore $e^{-i\gamma\hat{J}_z}$ commutes with $\frac{\partial}{\partial\gamma}$,

$$[e^{-i\gamma\hat{J}_z}, \tfrac{\partial}{\partial\gamma}] = 0. \tag{67}$$

We will also use that an operator $\hat{A}$ commutes with the exponentiation of an operator $\hat{B}$ if and only if $\hat{A}$ and $\hat{B}$ commute:

$$[\hat{A}, e^{\hat{B}}] = 0 \qquad (\text{iff } [\hat{A}, \hat{B}] = 0). \tag{68}$$

For example Eq. (68) [this document] implies that J_z commutes with $e^{i\gamma J_z}$. We will also use extensively that the derivative of an exponential of an operator can be written with either the residual exponential or the derivative of the exponent to the right. For example,

$$\frac{\partial}{\partial\beta}\left(e^{-i\beta\hat{J}_y}\right) = i\,\frac{\partial(\beta\hat{J}_y)}{\partial\beta}\,e^{-i\beta\hat{J}_y} = i\,e^{-i\beta\hat{J}_y}\,\frac{\partial(\beta\hat{J}_y)}{\partial\beta}, \tag{69}$$

which follows from taking the derivative of the expression $[\hat{J}_y, e^{-i\beta\hat{J}_y}] = 0$, which is true because of Eq. (65) [this document]. Finally we will often use that since the intrinsic state $|\Phi\rangle$ is assumed to be independent on the Euler angles (β, γ), any derivative operator gives zero when applied to $|\Phi\rangle$,

$$\frac{\partial}{\partial\beta}|\Phi\rangle = \frac{\partial}{\partial\gamma}|\Phi\rangle = \frac{\partial^2}{\partial\beta^2}|\Phi\rangle = \frac{\partial^2}{\partial\gamma^2}|\Phi\rangle = \frac{\partial^2}{\partial\beta\partial\gamma}|\Phi\rangle = \frac{\partial^2}{\partial\gamma\partial\beta}|\Phi\rangle = 0. \tag{70}$$

This will allow elimination of terms involving derivatives if the derivative operator can be commuted to the right to act on the intrinsic state.

C. Some Derivatives

Let's calculate some derivatives that will be needed, assuming that the Liebniz relation for derivatives of products

$$\frac{d}{dx}(AB) = \frac{d}{dx}(A)B + A\frac{d}{dx}(B) \tag{71}$$

holds also for possibly non-commuting operators. Then,

$$\begin{aligned}\frac{\partial}{\partial\beta}\left(e^{-i\beta\hat{J}_y}\right) &= -ie^{-i\beta\hat{J}_y}\frac{\partial}{\partial\beta}(\beta\hat{J}_y) = -ie^{-i\beta\hat{J}_y}\left(\hat{J}_y + \beta\frac{\partial\hat{J}_y}{\partial\beta}\right)\\ &= -ie^{-i\beta\hat{J}_y}\left[\hat{J}_y - i\beta\left(\cos\gamma\frac{\partial^2}{\partial\beta^2} + \frac{\sin\gamma}{\sin^2\beta}\frac{\partial}{\partial\gamma}\right)\right],\end{aligned} \tag{72}$$

where we have used that

$$\begin{aligned}\frac{\partial\hat{J}_y}{\partial\beta} &= i\frac{\partial}{\partial\beta}\left(-\cos\gamma\frac{\partial}{\partial\beta} + \cot\beta\cos\gamma\frac{\partial}{\partial\gamma}\right)\\ &= -i\left(\cos\gamma\frac{\partial^2}{\partial\beta^2} + \frac{\sin\gamma}{\sin^2\beta}\frac{\partial}{\partial\gamma}\right),\end{aligned} \tag{73}$$

from Eq. (55b) [this document]. In a similar manner,

$$\frac{\partial}{\partial\beta}\left(e^{-i\gamma\hat{J}_z}\right) = ie^{-i\gamma\hat{J}_z}\frac{\partial}{\partial\beta}(\gamma\hat{J}_z) = i\gamma e^{-i\gamma\hat{J}_z}\frac{\partial J_z}{\partial\beta}$$
$$= i\gamma e^{-i\gamma\hat{J}_z}\frac{\partial}{\partial\beta}\left(-i\frac{\partial}{\partial\gamma}\right) = \gamma e^{-i\gamma\hat{J}_z}\frac{\partial^2}{\partial\beta\partial\gamma}, \tag{74}$$

where we have used Eq. (55c) [this document] in line 2. Likewise,

$$\frac{\partial}{\partial\gamma}\left(e^{-i\beta\hat{J}_y}\right) = -ie^{-i\beta\hat{J}_j}\frac{\partial}{\partial\gamma}(\beta\hat{J}_y) = -ie^{-i\beta\hat{J}_j}\beta\frac{\partial\hat{J}_y}{\partial\gamma}$$
$$= e^{-i\beta\hat{J}_j}\beta\left(\sin\gamma\frac{\partial}{\partial\beta} + \cot\beta\cos\gamma\frac{\partial}{\partial\gamma} + \cot\beta\sin\gamma\frac{\partial^2}{\partial\gamma^2}\right), \tag{75}$$

where we have used Eq. (55b) [this document] to calculate the derivative

$$\frac{\partial\hat{J}_y}{\partial\gamma} = i\left[\sin\gamma\frac{\partial}{\partial\beta} + \cot\beta\left(\cos\gamma\frac{\partial}{\partial\gamma} + \sin\gamma\frac{\partial^2}{\partial\gamma^2}\right)\right]. \tag{76}$$

In a similar manner,

$$\frac{\partial}{\partial\gamma}\left(e^{-i\gamma\hat{J}_z}\right) = -ie^{-i\gamma\hat{J}_z}\frac{\partial}{\partial\gamma}(\gamma\hat{J}_y) = -ie^{-i\gamma\hat{J}_z}\left(\hat{J}_z - i\gamma\frac{\partial^2}{\partial\gamma^2}\right), \tag{77}$$

where we have used

$$\frac{\partial}{\partial\gamma}(\gamma\hat{J}_z) = \hat{J}_z + \gamma\frac{\partial\hat{J}_z}{\partial\gamma} = \hat{J}_z - i\gamma\frac{\partial^2}{\partial\gamma^2}, \tag{78}$$

which was deduced from Eq. (55c) [this document] upon setting $\hbar = 1$.

D. Berry Connections

The Berry connections for the Hilbert space of Eq. (8) are

$$A_\beta \equiv \langle\psi|i\partial_\beta|\psi\rangle \qquad A_\gamma \equiv \langle\psi|i\partial_\gamma|\psi\rangle, \tag{79}$$

where $\partial_\alpha \equiv \partial/\partial\alpha$. The wavefunctions $|\beta\gamma\rangle \equiv |\psi(\beta,\gamma)\rangle$ are

$$|\beta\gamma\rangle = e^{-i\beta\hat{J}_y}e^{-i\gamma\hat{J}_z}|\Phi\rangle \qquad \langle\beta\gamma| = \langle\Phi|e^{i\gamma\hat{J}_z}e^{i\beta\hat{J}_y}, \tag{80}$$

Using these wavefunctions, we then have

$$\frac{\partial}{\partial\gamma}|\beta\gamma\rangle = \frac{\partial}{\partial\gamma}\left(e^{-i\beta\hat{J}_y}e^{-i\gamma\hat{J}_z}\right)|\Phi\rangle = \frac{\partial}{\partial\gamma}\left(e^{-i\beta\hat{J}_y}\right)e^{-i\gamma\hat{J}_z}|\Phi\rangle + e^{-i\beta\hat{J}_y}\frac{\partial}{\partial\gamma}\left(e^{-i\gamma\hat{J}_z}\right)|\Phi\rangle$$
$$= e^{-i\beta\hat{J}_y}\beta\left(\sin\gamma\frac{\partial}{\partial\beta} + \cot\beta\cos\gamma\frac{\partial}{\partial\gamma} + \cot\beta\sin\gamma\frac{\partial^2}{\partial\gamma^2}\right)e^{-i\gamma\hat{J}_z}|\Phi\rangle - ie^{-i\beta\hat{J}_y}e^{-i\gamma\hat{J}_z}\left(\hat{J}_z - i\gamma\frac{\partial^2}{\partial\gamma^2}\right)|\Phi\rangle$$
$$= -ie^{-i\beta\hat{J}_y}\hat{J}_z e^{-i\gamma\hat{J}_z}|\Phi\rangle, \tag{81}$$

where in lines 2-3 manipulations like the following have been used to set all terms containing derivative operators to zero:

$$\sin\gamma\frac{\partial}{\partial\beta}\left(e^{-i\gamma\hat{J}_z}\right)|\Phi\rangle = \sin\gamma e^{-i\gamma\hat{J}_z}\frac{\partial}{\partial\beta}(\gamma\hat{J}_z)|\Phi\rangle$$
$$= \sin\gamma e^{-i\gamma\hat{J}_z}\gamma\frac{\partial}{\partial\beta}\left(-i\frac{\partial}{\partial\gamma}\right)|\Phi\rangle$$
$$= -i\gamma\sin\gamma e^{-i\gamma\hat{J}_z}\frac{\partial^2}{\partial\beta\partial\gamma}|\Phi\rangle = 0,$$

where Eqs. (55c), (69), and (70) [this document] have been used. By similar reasoning,

$$\cot\beta\cos\gamma\frac{\partial}{\partial\gamma}e^{-i\gamma\hat{J}_z}|\Phi\rangle = 0, \tag{82}$$

where we have used that from Eqs. (70) and (69) [this document],

$$\frac{\partial}{\partial\gamma}e^{-i\gamma\hat{J}_z}|\Phi\rangle = e^{-i\gamma\hat{J}_z}\frac{\partial}{\partial\gamma}|\Phi\rangle = 0. \tag{83}$$

Finally we have

$$\cot\beta\sin\gamma\frac{\partial^2}{\partial\gamma^2}e^{-i\gamma\hat{J}_z}|\Phi\rangle = \cot\beta\sin\gamma\frac{\partial}{\partial\gamma}\left(e^{-i\gamma\hat{J}_z}\frac{\partial}{\partial\gamma}\right)|\Phi\rangle = 0, \tag{84}$$

by virtue of Eq. (83) [this document], and

$$i\gamma\frac{\partial^2}{\partial\gamma^2}|\Phi\rangle = 0, \tag{85}$$

because of Eq. (70) [this document]. Therefore, all terms in Eq. (81) [this document] involving derivative operators vanish and we are left with

$$\frac{\partial}{\partial\gamma}|\beta\gamma\rangle = -ie^{-i\beta\hat{J}_y}\hat{J}_z e^{-i\gamma\hat{J}_z}|\Phi\rangle. \tag{86}$$

In a similar manner we find

$$\begin{aligned}\frac{\partial}{\partial\beta}|\beta\gamma\rangle &= \frac{\partial}{\partial\beta}\left(e^{-i\beta\hat{J}_y}e^{-i\gamma\hat{J}_z}\right)|\Phi\rangle \\ &= \left[\frac{\partial}{\partial\beta}\left(e^{-i\beta\hat{J}_y}\right)e^{-i\gamma\hat{J}_z} + e^{-i\beta\hat{J}_y}\frac{\partial}{\partial\beta}\left(e^{-i\gamma\hat{J}_z}\right)\right]|\Phi\rangle \\ &= -ie^{-i\beta\hat{J}_y}\left[\hat{J}_y - i\beta\left(\cos\gamma\frac{\partial^2}{\partial\beta^2} + \frac{\sin\gamma}{\sin^2\beta}\frac{\partial}{\partial\gamma}\right)\right] \\ &= -i\hat{J}_y e^{-i\beta\hat{J}_y}e^{-i\gamma\hat{J}_z}|\Phi\rangle.\end{aligned} \tag{87}$$

The results in Eqs. (81) and (87) [this document] may then be used to calculate the Berry connections A_β and A_γ from

$$A_\beta = \langle\beta\gamma|i\tfrac{\partial}{\partial\beta}|\beta\gamma\rangle \qquad A_\gamma = \langle\beta\gamma|i\tfrac{\partial}{\partial\gamma}|\beta\gamma\rangle.$$

From Eq. (87) [this document]

$$\frac{\partial}{\partial\beta}|\beta\gamma\rangle = -i\hat{J}_y e^{-i\beta\hat{J}_y}e^{-i\gamma\hat{J}_z}|\Phi\rangle, \tag{88}$$

$$\frac{\partial}{\partial\gamma}|\beta\gamma\rangle = -ie^{-i\beta\hat{J}_y}\hat{J}_z e^{-i\gamma\hat{J}_z}|\Phi\rangle, \tag{89}$$

where $|\Phi\rangle$ is assumed not to depend on the Euler angles (β,γ). The connection A_β is given by

$$\begin{aligned}A_\beta = \langle\beta\gamma|i\tfrac{\partial}{\partial\beta}|\beta\gamma\rangle &= i(-i)\langle\Phi|e^{i\gamma\hat{J}_z}e^{i\beta\hat{J}_y}\hat{J}_y e^{-i\beta\hat{J}_y}e^{-i\gamma\hat{J}_z}|\Phi\rangle \\ &= \langle\Phi|e^{i\gamma\hat{J}_z}e^{i\beta\hat{J}_y}e^{-i\beta\hat{J}_y}\hat{J}_y e^{-i\gamma\hat{J}_z}|\Phi\rangle \\ &= \langle\Phi|e^{i\gamma\hat{J}_z}\hat{J}_y e^{-i\gamma\hat{J}_z}|\Phi\rangle = \langle\Phi|\hat{J}_2|\Phi\rangle,\end{aligned} \tag{90}$$

where we've used Eq. (88) [this document], that $[\hat{A},e^{\hat{B}}]=0$ only if $[\hat{A},\hat{B}]=0$ from Eq. (68) [this document], and Eq. (60) [this document]. Likewise, the connection A_γ is

$$\begin{aligned}A_\gamma = \langle\beta\gamma|i\tfrac{\partial}{\partial\gamma}|\beta\gamma\rangle &= i(-i)\langle\Phi|e^{i\gamma\hat{J}_z}e^{i\beta\hat{J}_y}e^{-i\beta\hat{J}_y}\hat{J}_z e^{-i\gamma\hat{J}_z}|\Phi\rangle \\ &= \langle\Phi|e^{i\gamma\hat{J}_z}\hat{J}_z e^{-i\gamma\hat{J}_z}|\Phi\rangle = \langle\Phi|\hat{J}_z|\Phi\rangle,\end{aligned} \tag{91}$$

where Eq. (89) [this document] was used.

E. Berry Curvature

From Eq. (16), we need $\partial A_\beta/\partial\gamma$ to evaluate the integral of Berry curvature over Hilbert space. From Eq. (90) [this document],

$$\begin{aligned}\frac{\partial A_\beta}{\partial\gamma} &= \frac{\partial}{\partial\gamma}\langle\Phi|e^{i\gamma\hat{J}_z}\hat{J}_y e^{-i\gamma\hat{J}_z}|\Phi\rangle \\ &= \left\langle\Phi\left|\frac{\partial}{\partial\gamma}\left(e^{i\gamma\hat{J}_z}\right)\hat{J}_y e^{-i\gamma\hat{J}_z}\right|\Phi\right\rangle \quad \text{(Term 1)} \\ &+ \left\langle\Phi\left|e^{i\gamma\hat{J}_z}\frac{\partial\hat{J}_y}{\partial\gamma}e^{-i\gamma\hat{J}_z}\right|\Phi\right\rangle \quad \text{(Term 2)} \\ &+ \left\langle\Phi\left|e^{i\gamma\hat{J}_z}\hat{J}_y\frac{\partial}{\partial\gamma}\left(e^{-i\gamma\hat{J}_z}\right)\right|\Phi\right\rangle \quad \text{(Term 3)},\end{aligned} \tag{92}$$

where $|\Phi\rangle$ is assumed to be independent of (β,γ). Let's now evaluate each of the three terms in Eq. (92) [this document]. For the first term,

$$\begin{aligned}\text{Term 1} &= \left\langle\Phi\left|\frac{\partial}{\partial\gamma}\left(e^{i\gamma\hat{J}_z}\right)\hat{J}_y e^{-i\gamma\hat{J}_z}\right|\Phi\right\rangle \\ &= \left\langle\Phi\left|ie^{i\gamma\hat{J}_z}\left(\hat{J}_z-\gamma\frac{\partial^2}{\partial\gamma^2}\right)\hat{J}_y e^{-i\gamma\hat{J}_z}\right|\Phi\right\rangle \\ &= \left\langle\Phi\left|ie^{i\gamma\hat{J}_z}\hat{J}_z\hat{J}_y e^{-i\gamma\hat{J}_z}\right|\Phi\right\rangle + \left\langle\Phi\left|e^{i\gamma\hat{J}_z}\gamma\frac{\partial^2}{\partial\gamma^2}\hat{J}_y e^{-i\gamma\hat{J}_z}\right|\Phi\right\rangle \\ &= \left\langle\Phi\left|ie^{i\gamma\hat{J}_z}\hat{J}_z\hat{J}_y e^{-i\gamma\hat{J}_z}\right|\Phi\right\rangle + \left\langle\Phi\left|e^{i\gamma\hat{J}_z}\gamma\frac{\partial}{\partial\gamma}\left[\frac{\partial}{\partial\gamma}\left(\hat{J}_y e^{-i\gamma\hat{J}_z}\right)\right]\right|\Phi\right\rangle \\ &= \left\langle\Phi\left|ie^{i\gamma\hat{J}_z}\hat{J}_z\hat{J}_y e^{-i\gamma\hat{J}_z}\right|\Phi\right\rangle,\end{aligned} \tag{93}$$

where in line 2 Eq. (77) [this document] was used and the second term of line 4 was eliminated by

$$\begin{aligned}\left\langle\Phi\left|e^{i\gamma\hat{J}_z}\gamma\frac{\partial}{\partial\gamma}\left[\frac{\partial}{\partial\gamma}\left(\hat{J}_y e^{-i\gamma\hat{J}_z}\right)\right]\right|\Phi\right\rangle &= \left\langle\Phi\left|e^{i\gamma\hat{J}_z}\gamma\frac{\partial}{\partial\gamma}\left[\left(\frac{\partial\hat{J}_y}{\partial\gamma}\right)e^{-i\gamma\hat{J}_z}+\hat{J}_y\frac{\partial}{\partial\gamma}\left(e^{-i\gamma\hat{J}_z}\right)\right]\right|\Phi\right\rangle \\ &= \left\langle\Phi\left|e^{i\gamma\hat{J}_z}\gamma\frac{\partial}{\partial\gamma}\left[\left(\frac{\partial\hat{J}_y}{\partial\gamma}\right)e^{-i\gamma\hat{J}_z}+\hat{J}_y\left(e^{-i\gamma\hat{J}_z}\right)\frac{\partial}{\partial\gamma}\right]\right|\Phi\right\rangle \\ &= \left\langle\Phi\left|e^{i\gamma\hat{J}_z}\gamma\frac{\partial}{\partial\gamma}\left[\left(\frac{\partial\hat{J}_y}{\partial\gamma}\right)e^{-i\gamma\hat{J}_z}\right]\right|\Phi\right\rangle \\ &= \left\langle\Phi\left|e^{i\gamma\hat{J}_z}i\gamma\frac{\partial}{\partial\gamma}\left[\left(\sin\gamma\frac{\partial}{\partial\beta}+\cot\beta\cos\gamma\frac{\partial}{\partial\gamma}+\cot\beta\sin\gamma\frac{\partial^2}{\partial\gamma^2}\right)e^{-i\gamma\hat{J}_z}\right]\right|\Phi\right\rangle = 0,\end{aligned} \tag{94}$$

where in line 2 we have used Eq. (67) [this document], in line 3 we have used Eq. (70) [this document], in line 4 we have used Eq. (70) [this document], and in line 4 the partial derivative factors can all be brought to the right to act on $|\Phi\rangle$ and give zero by commuting with the exponential factor $\exp(-i\gamma\hat{J}_z)$:

- The exponential $\exp(-i\gamma\hat{J}_z)$ does not depend on β so it commutes with $\partial/\partial\beta$.
- From Eq. (67) [this document], $\exp(-i\gamma\hat{J}_z)$ commutes with $\partial/\partial\gamma$.
- In the last term of line 5,

$$\frac{\partial^2}{\partial\gamma^2}e^{-i\gamma\hat{J}_z} = \frac{\partial}{\partial\gamma}\left[\frac{\partial}{\partial\gamma}e^{-i\gamma\hat{J}_z}\right] = \frac{\partial}{\partial\gamma}\left[e^{-i\gamma\hat{J}_z}\frac{\partial}{\partial\gamma}\right]$$

  where Eq. (67) [this document] was used.

From Eq. (70) [this document], the partial derivative factors then all give zero when operating on the intrinsic state $|\Phi\rangle$ and the entire contribution of Eq. (94) [this document] to Term 1 vanishes. By similar means, Term 2 vanishes identically,

$$\begin{aligned}
\text{Term 2} &= \left\langle \Phi \left| e^{i\gamma\hat{J}_z} \left(\frac{\partial \hat{J}_y}{\partial \gamma} \right) e^{-i\gamma\hat{J}_z} \right| \Phi \right\rangle \\
&= \left\langle \Phi \left| e^{i\gamma\hat{J}_z} i \left(\sin\gamma \frac{\partial}{\partial\beta} + \cot\beta\cos\gamma \frac{\partial}{\partial\gamma} + \cot\beta \sin\gamma \frac{\partial^2}{\partial\gamma^2} \right) e^{-i\gamma\hat{J}_z} \right| \Phi \right\rangle \\
&= \left\langle \Phi \left| e^{i\gamma\hat{J}_z} i \left(\sin\gamma e^{-i\gamma\hat{J}_z} \frac{\partial}{\partial\beta} + \cot\beta\cos\gamma e^{-i\gamma\hat{J}_z} \frac{\partial}{\partial\gamma} + \cot\beta\sin\gamma \frac{\partial}{\partial\gamma} \left[e^{-i\gamma\hat{J}_z} \frac{\partial}{\partial\gamma} \right] \right) \right| \Phi \right\rangle = 0, \qquad (95)
\end{aligned}$$

where Eq. (76) [this document] was used to expand $\frac{\partial \hat{J}_y}{\partial\gamma}$ in line 2, and in line 3 the partial derivative factors can all be brought to the right to act on $|\Phi\rangle$ by commuting with the exponential factor $\exp(-i\gamma\hat{J}_z)$ on their right in the same manner as for Term 1:

- The exponential $\exp(-i\gamma\hat{J}_z)$ does not depend on β so it commutes with $\partial/\partial\beta$.
- From Eq. (67) [this document], $\exp(-i\gamma\hat{J}_z)$ commutes with $\partial/\partial\gamma$.
- In the last term of line 2,

$$\frac{\partial^2}{\partial\gamma^2} e^{-i\gamma\hat{J}_z} = \frac{\partial}{\partial\gamma}\left[\frac{\partial}{\partial\gamma} e^{-i\gamma\hat{J}_z} \right] = \frac{\partial}{\partial\gamma}\left[e^{-i\gamma\hat{J}_z} \frac{\partial}{\partial\gamma} \right],$$

  where Eq. (67) [this document] was used.

From Eq. (70) [this document], the partial derivative factors then all give zero when operating on the intrinsic state $|\Phi\rangle$ and Term 2 vanishes. Proceeding in a similar way, Term 3 gives

$$\begin{aligned}
\text{Term 3} &= \left\langle \Phi \left| e^{i\gamma\hat{J}_z} \hat{J}_y \frac{\partial}{\partial\gamma} \left(e^{-i\gamma\hat{J}_z} \right) \right| \Phi \right\rangle \\
&= \left\langle \Phi \left| e^{i\gamma\hat{J}_z} \hat{J}_y (-i) \left(\hat{J}_z - i\gamma \frac{\partial^2}{\partial\gamma^2} \right) e^{-i\gamma\hat{J}_z} \right| \Phi \right\rangle \\
&= -i \left\langle \Phi \left| e^{i\gamma\hat{J}_z} \hat{J}_y \hat{J}_z e^{-i\gamma\hat{J}_z} \right| \Phi \right\rangle - \left\langle \Phi \left| e^{i\gamma\hat{J}_z} \hat{J}_y \gamma \frac{\partial^2}{\partial\gamma^2} e^{-i\gamma\hat{J}_z} \right| \Phi \right\rangle \\
&= -i \left\langle \Phi \left| e^{i\gamma\hat{J}_z} \hat{J}_y \hat{J}_z e^{-i\gamma\hat{J}_z} \right| \Phi \right\rangle - \left\langle \Phi \left| e^{i\gamma\hat{J}_z} \hat{J}_y \gamma \frac{\partial}{\partial\gamma} \left(e^{-i\gamma\hat{J}_z} \frac{\partial}{\partial\gamma} \right) \right| \Phi \right\rangle \\
&= -i \langle \Phi | e^{i\gamma\hat{J}_z} \hat{J}_y \hat{J}_z e^{-i\gamma\hat{J}_z} | \Phi \rangle, \qquad (96)
\end{aligned}$$

where Eq. (67) [this document] was used in the second term of line 3 to bring $\partial/\partial\gamma$ to the right and the second term in line 4 vanishes because of Eq. (70) [this document]. Inserting the results (93), (95), and (96) [this document] into Eq. (92) [this document] leads to

$$\begin{aligned}
\frac{\partial A_\beta}{\partial\gamma} &= \frac{\partial}{\partial\gamma} \langle \Phi | e^{i\gamma\hat{J}_z} \hat{J}_y e^{-i\gamma\hat{J}_z} | \Phi \rangle \\
&= \langle \Phi | i\hat{J}_z e^{i\gamma\hat{J}_z} \hat{J}_y e^{-i\gamma\hat{J}_z} | \Phi \rangle - i \langle \Phi | e^{i\gamma\hat{J}_z} \hat{J}_y \hat{J}_z e^{-i\gamma\hat{J}_z} | \Phi \rangle \\
&= i \langle \Phi | e^{i\gamma\hat{J}_z} \hat{J}_z \hat{J}_y e^{-i\gamma\hat{J}_z} | \Phi \rangle - i \langle \Phi | e^{i\gamma\hat{J}_z} \hat{J}_y \hat{J}_z e^{-i\gamma\hat{J}_z} | \Phi \rangle \\
&= i \langle \Phi | e^{i\gamma\hat{J}_z} (\hat{J}_z \hat{J}_y - \hat{J}_y \hat{J}_z) e^{-i\gamma\hat{J}_z} | \Phi \rangle \\
&= i \langle \Phi | e^{i\gamma\hat{J}_z} [\hat{J}_z, \hat{J}_y] e^{-i\gamma\hat{J}_z} | \Phi \rangle \\
&= \langle \Phi | e^{i\gamma\hat{J}_z} \hat{J}_x e^{-i\gamma\hat{J}_z} | \Phi \rangle, \qquad (97)
\end{aligned}$$

where in the second line we have used the usual formula for the derivative of a product and in the last line we have used that the $\hat{J}_i$ are generators of angular momentum that obey an SU(2) Lie algebra $[\hat{J}_i, \hat{J}_j] = i\varepsilon_{ijk}\hat{J}_k$, where ε_{ijk} is the completely antisymmetric rank-2 tensor. Thus, integration of the Berry curvature over the Hilbert space has recovered the SU(2) Lie algebra of the rotor angular momentum operators. This gives Eq. (97) [present document] for $\partial A_\beta/\partial\gamma$.

Then the Berry curvature integrated over the Hilbert-space manifold $\Gamma^{\gamma\beta}$ is

$$\begin{aligned}\Gamma^{\gamma\beta} \equiv \int_S \Omega\, dA &= \int_{\gamma_i}^{\gamma_f} d\gamma \int_0^{\pi} d\beta \sin\beta \left(\frac{\partial A_\gamma}{\partial \beta} - \frac{\partial A_\beta}{\partial \gamma} \right) \\ &= -\int_{\gamma_i}^{\gamma_f} d\gamma \int_0^{\pi} d\beta \sin\beta \left(\frac{\partial A_\beta}{\partial \gamma} \right) \\ &= -\int_{\gamma_i}^{\gamma_f} d\gamma \frac{\partial}{\partial \gamma} \int_0^{\pi} d\beta \sin\beta A_\beta \\ &= -\int_{\gamma_i}^{\gamma_f} d\gamma \frac{\partial \phi^\beta}{\partial \gamma} \\ &= -\int_{\gamma_i}^{\gamma_f} d\phi^\beta \\ &= \phi^\beta(\gamma_i) - \phi^\beta(\gamma_f), \end{aligned} \tag{98}$$

where in line 3 the order of integration and differentiation has been switched, and the Berry phase $\phi^\beta(\gamma)$ evaluated on a closed path in β at fixed γ has been defined by

$$\begin{aligned}\phi^\beta(\gamma) &\equiv \int_0^{\pi} d\beta \sin\beta A_\beta \\ &= \langle\Phi| e^{i\gamma\hat{J}_z} \hat{J}_y e^{-i\gamma\hat{J}_z} |\Phi\rangle \int_0^{\pi} d\beta \sin\beta \\ &= 2\langle\Phi| e^{i\gamma\hat{J}_z} \hat{J}_y e^{-i\gamma\hat{J}_z} |\Phi\rangle = 2\langle\Phi|\hat{J}_2|\Phi\rangle, \end{aligned} \tag{99}$$

where Eq. (90) [this document] has been used and in the second step the intrinsic state $|\Phi\rangle$ has been assumed to be independent of β. This result gives Eq. (19) of the main manuscript.

From Eq. (17), the volume of the 2D Hilbert space is $V_{\rm H} = 4\pi$. Thus, dividing both sides of Eq. (21) by $V_{\rm H}$, the Chern theorem takes the form

$$\begin{aligned}\overline{\Gamma}^{\gamma\beta} \equiv \frac{\Gamma^{\gamma\beta}}{V_{\rm H}} &= \frac{2\langle\Phi| e^{i\gamma_{\rm i}\hat{J}_z} \hat{J}_y e^{-i\hat{J}_z} |\Phi\rangle - 2\langle\Phi| e^{i\gamma_{\rm f}\hat{J}_z} \hat{J}_y e^{-i\gamma_{\rm f}\hat{J}_z} |\Phi\rangle}{4\pi} \\ &= \frac{1}{2\pi} \left[\left\langle\left\langle \Phi| e^{i\gamma_{\rm i}\hat{J}_z} \hat{J}_y e^{-i\gamma_{\rm i}\hat{J}_z} |\Phi\right\rangle\right\rangle - \left\langle\left\langle \Phi| e^{i\gamma_{\rm f}\hat{J}_z} \hat{J}_y e^{-i\gamma_{\rm f}\hat{J}_z} |\Phi\right\rangle\right\rangle \right] \\ &= \frac{1}{2} C_1 = \frac{1}{2} \times \{0, 1, 2, 3, \ldots\}, \end{aligned} \tag{100}$$

where C_1 is a first Chern number and the double-bracket notation

$$\left\langle\left\langle A|B|C\right\rangle\right\rangle \equiv \frac{\langle A|B|C\rangle}{V_{\rm H}} \tag{101}$$

indicates an average of a matrix element $\langle A|B|C\rangle$ over the Hilbert-space volume $V_{\rm H}$. This gives Eq. (23) of the main manuscript.